Supporting Information

Table of Contents

Experimental Procedures

Synthesis

Common reagents and solvents were purchased from Sigma-Aldrich (Schnelldorf, Germany), Fluka (Buchs, Switzerland), Merck (Darmstadt, Germany) and Fisher Scientific (Schwerte, Germany) and used without further purification. Acetonitrile (ACN) and acetone were dried with molecular sieve (3 Å) and stored under argon atmosphere. Microwave assisted reactions were carried out on a MLS-Ethos 1600 system from MLS-GmbH (Leutkirch, Germany). Reaction control was done on TLC plates SIL G-25 pre-coated with fluorescent indicator 254 nm from Macherey-Nagel (Düren, Germany) and spots were detected under UV light or by iodine vapor.
NMR measurements were performed with a Bruker Avance III 400 MHz spectrometer from Bruker (Karlsruhe, Germany) and the data were processed with the TopSpin 3.0 software from Bruker. Brown glass and standard NMR tubes 5 mm (400 MHz) were purchased from Norell (Landisville, PA). For mass spectrometry data the compounds were dissolved in HPLC-grade methanol, injected into a LC system (series 1200), ionized by electrospray ionization (ESI) and detected by an ion trap G2445D from Agilent (Waldbronn, Germany). For high-resolution MS a micrOTOF-Q III detector with electrospray ionization (ESI) from Bruker was used. The melting point was determined by dynamic scanning calorimetry with a DSC 8000 from Perkin Elmer (Waltham, Massachusetts).

UV light irradiation

UV-light with a wavelength of λ = 365 nm was irradiated by a UV-LED smart lamp and 100% intensity from Opsytec (Ettlingen, Germany). A LED lamp with cooling element was chosen to avoid thermal irradiation and the optic “wide" was used. The distance lamp to sample was 5 cm resulting in an irradiance of about 650 mW/cm^2. The exposure time was 15 min unless otherwise noted.

Blue light irradiation

Blue-light with a wavelength of λ = 445 nm was irradiated by a LED smart lamp and 100% intensity from Opsytec (Ettlingen, Germany). A LED lamp with cooling element was chosen to avoid thermal irradiation and the optic “wide" was used. The distance from lamp to sample was 5 cm. The exposure time was 15 min unless otherwise noted.

Images and movies

Images and movies were recorded on BX40 microscope from Olympus (Tokyo, Japan) with a Moticam 3 MP from Motic (Wetzlar, Germany) at room temperature.

HPLC analysis

Analytical HPLC analyses were performed using an Agilent Technologies 1100 series systems (Waldbronn, Germany) consisting of a binary pump, a degasser, an autosampler, a column thermostat and a diode-array UV detector. Millipore water was obtained by in-house Millipore system from Merck (Darmstadt, Germany).

Determination of the *cis-trans* ratio

Solutions of the compounds (800 µM) in a mixture of water and acetonitrile (40:60) were analyzed without (dark) and immediately after UV light exposure (15 min) by HPLC analysis. The separation was carried out with an isocratic method using 40% A: water with 0.1% trifluoroacetic acid and 60% B: acetonitrile with 0.1% trifluoroacetic acid with a flow of 1 mL/min and using an Synergy Max-RP column (4.6 x 150 mm, 4 µm, 80 Å) from Phenomenex (Aschaffenburg, Germany) with a pre-column. The injection volume was 50 µL and the column thermostat was kept at 25 °C. For the ammonium salts (6,4,N,3-Br / 6,4,N,3-S) the run time of the method was 40 min and 18 min for the phosphonium salts (6,4,P,1-Br / 6,4,P,1-I). The *cis*-to-*trans* ratio was determined by the area under the peaks of the HPLC chromatograms using the detector wavelength 235 nm (isosbestic point of *the cis* and *trans* form).

Apparent solubility in water

In brief, for solubility measurements a suspension in millipore water was shaken at 400 rpm at 22 °C for the duration as indicated in the respected figure and by an Eppendorf thermomixer (Hamburg, Germany). The measurements were performed in triplicate in dark and under UV light irradiation. The samples were taken at different time points and centrifuged by an EBA 12 centrifuge from Hettich (Tuttlingen, Germany). The supernatant was diluted with water and acetonitrile (50:50, V:V) and analyzed by HPLC as described before for the 6,4,P,1-I. For 6,4,N,3-S the separation was carried out using a Synergy Max-RP column (4.6 x 150 mm, 4 µm) from Phenomenex (Aschaffenburg, Germany) and a gradient of A: 20 mM aqueous potassium dihydrogen phosphate buffer pH 2.5 and B: methanol with a flow of 1 mL/min and applying a wavelength of 237 nm. The elution started isocratic 45:55 (A:B, v/v) from 0 - 7 min, going to 10:90 (A:B, v/v) within 7 - 10 min, kept isocratic from 10 - 15 min 10:90 (A:B, v/v), and conditioned with 45:55 (A:B, v/v) for 2 min. The injection volume was 20 µL and the column thermostat was kept at 25 °C.

Franz cell assays with Strat-M®-Membrane

In vitro permeation studies were carried out with jacketed Franz vertical diffusion cells with a standard orifice diameter of 20 mm and a receptor volume of 15 mL. The receptor fluid was phosphate-buffered saline (PBS) solution pH 7.4, the temperature was set to 32 °C and the stirring speed was 300 rpm. The Strat-M®-membranes were placed between the donor and receptor chamber and the equilibration time was 2 h. 800 µL of the test solutions was pipetted on the membrane surface and the donor chamber was covered using Parafilm® to prevent evaporation of the water during the experiment. After 6, 24, 48 and 72 hours, 400 µL of the receptor fluid was withdrawn for analysis and equal amounts of fresh, pre-warmed PBS was added after each sampling procedure. All experiments were performed in triplicate and under the exclusion of light. The samples were centrifuged at 13.000 rpm for 10 min and the supernatant was analyzed using HPLC analysis as described before. The injection volume was 20 µL and the column thermostat was kept at 25 °C.

Isothermal titration calorimetry (ITC)

The measurements were carried out on a MicroCal™ Calorimeter iTC_{200} from GE Healthcare (Northampton, MA) by successive addition of concentrated solutions of the compound in Millipore water to the sample cell filled with Millipore water (200 µL cell size). 40 µL of the solution was injected in 2 µL steps (duration 0.8) into the sample cell and the heat differences were measured compared to the reference cell filled with the same solvent. The spacing was 150 s and the stirring rate was 250 rpm. The ITC data were analyzed with the model fitting One Set of Sites in Origin 7.0 from OriginLab Cooperation (Northampton, MA). The concentration of the stock solutions filled in the syringe was 800 µM for dark (not irradiated) and 3200 µM for the UV-irradiated samples, respectively.

Dynamic light scattering (DLS)

The samples were prepared in Millipore water, filtrated with mini-filters Nalgene® (0.2 µm) from Thermo Fisher Scientific (Waltham, MA) and equilibrated overnight (> 12 h). The DLS measurements were performed by using a Delsa Nano HC particle analyzer from Beckman Coulter (Brea, CA) at 25 °C in water and backscattering at an angle of 165°. The samples were filled in disposable UV-cuvettes (1.5 mL) from Brand (Wertheim, Germany). The density of the solution was measured by a density meter DMA 4100M and a microviscosimeter Lovis 2000 M of Anton Paar GmbH (Scharnhausen, Germany). The refractive index was set to 1.333 and the viscosity to 1.4600. The measurements were performed in triplicate with an accumulation of 70 scans and the data were analyzed by the CONTIN algorithm.

^{1}H nuclear magnetic resonance (NMR) measurements in deuterated water

For each measurement brown glass NMR tubes were used for ambient light protection. The samples were prepared analogous to the DLS measurements, but deuterated water was used instead of water. The samples were filled in the NMR tubes not irradiated (dark) and after UV-light irradiation. For ^{1}H NMR following acquisition parameters were applied: 128 scans, at a temperature of 300 K, flip angle of 30°, spectral width of 20.55 ppm, and transmitter offset of 6.175 ppm. The acquisition time was set to 3.985 seconds followed by a relaxation delay of 1.0 seconds with collection of 64,000 data points at a sample spinning frequency of 20 Hz. Processing parameters were set to an exponential line broadening window function of 0.3 Hz, an automatic baseline correction and manual phasing. The spectra were referenced to the external standard of 0.05% 3-(trimethylsilyl)propionic-2,2,3,3-d_4 sodium salt (TSP-d_4) in D_2O filled in a coaxial insert tube.

UV-VIS measurements

The UV-VIS spectra were recorded by an UV-VIS spectrometer Genesys 10S from Thermo Scientific (Waltham, MA). The samples were filled in a QS quartz cuvette (10 mm) from Hellma Analytics (Müllheim, Germany) and the spectra were recorded in the range from 600 to 200 nm.

X-ray powder diffraction

For X-ray powder diffractometry the powdered samples were filled in a capillary and analyzed with a Bruker Discover D8 powder diffractometer (Karlsruhe, Germany) using Cu-K_α radiation (unsplit $K\alpha_1$+$K\alpha_2$ doublet, mean wavelength λ = 154.19 pm) at a power of 40 kV and 40 mA, a focusing Goebel mirror and a 1.2 mm microfocus alignment. The scattered X-ray beam went through a receiving slit with 7.5 mm opening, 2.5° axial Soller slit and detection was performed with a LynxEye-1D-Detector (Bruker AXS) using the full detector range of 192 channels. Measurements were done in reflection geometry in coupled two theta/theta mode with a step size of 0.025° in 2θ and 0.25 s measurement time per step in the range of 5 – 40° (2θ). Data collection and processing was carried out with the software packages DIFFRAC.Suite and DIFFRAC.EVA 2.1 from Bruker (Karlsruhe, Germany).

Differential Scanning Calorimetry (DSC)

Differential Scanning Calorimetry (DSC) was performed on a DSC 8000 instrument from Perkin Elmer (Waltham, MA). The thermogram of 6,4,P,1-I (dark) was recorded with a heating rate of 20 °C/min from -50 to 200 °C followed by cooling with a rate of 50 °C/min from 200 °C to -50 °C. The DSC thermogram of the amorphous room-temperature ionic liquid after UV-light irradiation of the powdered sample of 6,4,P,1-I was measured with a cooling rate of 5 °C/min from 20 °C to -50 °C followed by heating with a rate of 5 °C/min from -50 °C to 20 °C. Between 20 °C and 160 °C the heating rate was reduced from 5 °C/min to 0.2 °C/min in order to follow the slow recrystallization process due the thermally induced *cis*-to-*trans* isomerization.

Cryo-transmission electron microscopy (cryo-TEM)

Holey carbon coated copper grids Quantifoil R 1.2/1.3 (400 mesh) from Quantifoil Micro Tools GmbH (Jena, Germany) were glow discharged for 2 min with a plasma cleaner PDC-002 from Harrick Plasma (Ithaca, New York) on medium setting and used within 1 hour. Samples (3.5 µL) were applied on the glow discharged grids, incubated for 45 seconds at 25 °C with 100% humidity, blotted from both sides for 4 seconds with blot force 0 and plunged in liquid ethane using a Vitrobot IV from FEI (Eindhoven, The Netherlands). Samples were transferred into a Titan Krios G3 electron microscope from Thermo Fisher – FEI and movies were recorded at 300 kV with a Falcon III camera in integrating mode. The sample was parallel illuminated with a beam diameter of 1000 nm at a spot size 5 in nanoprobe mode. A defocus of 3 µm was used and a total dose of 6000 e/nm^2. A nominal magnification of 75,000 was used which corresponding to a calibrated pixel size of 0.10635 nm per pixel. The C2 aperture was set to 70 µm and the objective aperture to 100 µm. The EPU software was used for data acquisition and frame alignment.

Small-angle X-ray scattering (SAXS)

A Bruker nanostar device with a Vantec 2000 detector and microfocus X-ray tube (Cu, unsplit $K\alpha_1$+$K\alpha_2$ doublet, mean wavelength λ = 1.54184 Å) from Incoatec (Geesthacht, Germany) was used for small-angle X-ray scattering analysis. The samples were filled in Mark-tubes from Hilgenberg (Malsfeld, Germany) and the distance to the detector was 67 cm. The sample was measured not irradiated (dark) and after 75 min irradiation with UV light.

Scanning laser transformation

A homemade inverted microscope with steerable inputs from a range of lasers was used to study the response of the gel of 6,4,P,1-I to focused illumination. The input laser was steered by computer-controlled galvanometer mirrors. Available lasers included a Kapteyn-Murnane Griffin ultrashort pulsed Ti:Sapphire laser tunable from 720 to 860 nm, a 488 nm semiconductor laser (Toptica iBeam Smart), 532 nm from the residual pump (Verdi V10, Coherent) for the ultrashort laser, and 633 nm from a HeNe laser. In the results presented here used a 60x objective with 0.65 NA. The gel was placed between a glass slide and a coverslip (with coverslips used as spacers) and sealed with epoxy. A LabVIEW computer interface was used to steer the laser, monitor laser power and collect images using a Basler Ace acA640-750um USB camera.

Molecular modeling

The starting structure for the cylindrical micelle of *trans* P^+-azobenzene was modeled in a similar way as suggested by previous publications.[1-2] Nine molecules of *trans* P^+-azobenzene were positioned circularly with a distance of about 4 Å to the central axis of the

micelle and an angle of approximately 40° to each other in a single layer, with the phosphonium moiety facing outwards. A copy of the slice was rotated along by 20° and moved approximately 5 Å along the z-axis. The two layers were then duplicated five times to generate a micelle of ten slices, resulting in 90 molecules. The same number of Ibuprofen molecules was randomly placed in the vicinity of the micelle. Solvation along the x- and y-axes of the model with TIP3P water was performed using tleap from AmberTools18,[4] with a minimum distance of 50 Å of azobenzene and Ibuprofen molecules to the simulation box border. The simulation box (22 x 22 x 7 nm^3) contained 99131 water molecules. This setup prevents interaction with micelles of neighboring boxes and also leads to an infinitely long cylinder along the z-axis over periodic boundaries.

Additionally, a model of a small spherical micelle of *cis* P^+-azobenzene was built. 36 *cis* P^+-azobenzene molecules together with 36 Ibuprofen molecules were randomly put together in a globular formation and also solvated with TIP3P water (in all directions, creating a cubic box), ensuring a minimum distance of 30 Å of the molecules to the borders. All systems were built in MOE (Molecular Operating Environment 2018.01).[5] Partial charges for azobenzene and Ibuprofen were derived with Gaussian 09 Rev. C.01[6] (Hartree-Fock level of theory with 6-31G* basis set and GAFF2[7] force field files were generated using *antechamber* and *parmchk*.[4] Parameters for azobenzene were then modified according to a previous publication.[8] Calculation of mean values of several bond distances, angles and dihedrals from 50 ns simulations of single molecules (*trans* and *cis*) in explicit solvent agreed with values from QM calculations.[9] NAMD 2.13[10] with a time step of 2 fs was used for all simulations. Periodic boundary conditions with the particle mesh Ewald method (cutoff 1.2 nm)[11] for electrostatic interactions were applied. Semi-isotropic coupling was used to allow for fluctuations along the z-axis, independent from the x- and y-axes. The cylindrical micelle was equilibrated first by minimization for 10,000 steps and subsequent heating-up from 100 to 300 K over the course of 500 ps. Harmonic constraints on Ibuprofen and azobenzene atoms were applied. These constraints were then gradually reduced over 1.6 ns. The temperature was held constant by Langevin dynamics and pressure was controlled with the Nosé-Hoover Langevin piston method (1.01325 bar). After simulation of another nanosecond in NPT, a production run was performed for 20 ns. Coordinates were saved every picosecond.

The simulation of the spherical *cis* micelle was performed equivalently, except for the semi-isotropic coupling. For the calculation of the packing parameter, according to Israelachvili,[12] several properties from the simulation of the cylindrical micelle (from the last 5 ns) were analyzed (**Table S2**). We computed the van-der-Waals area of the polar head groups, the maximum length of the hydrophobic tails, as well as the volumes for the lipophilic part. Calculations for radii of gyration, distances and length measurements of molecules were done using *cpptraj*.[4] The surface area of the polar head groups was calculated using the *measure sasa* command in VMD-1.9.2,[13] ignoring intra- and intermolecular contacts of azobenzene and Ibuprofen. Volumes were calculated within MOE. Structure figures were generated with VMD-1.9.2.

Synthesis of the photoswitchable counterions

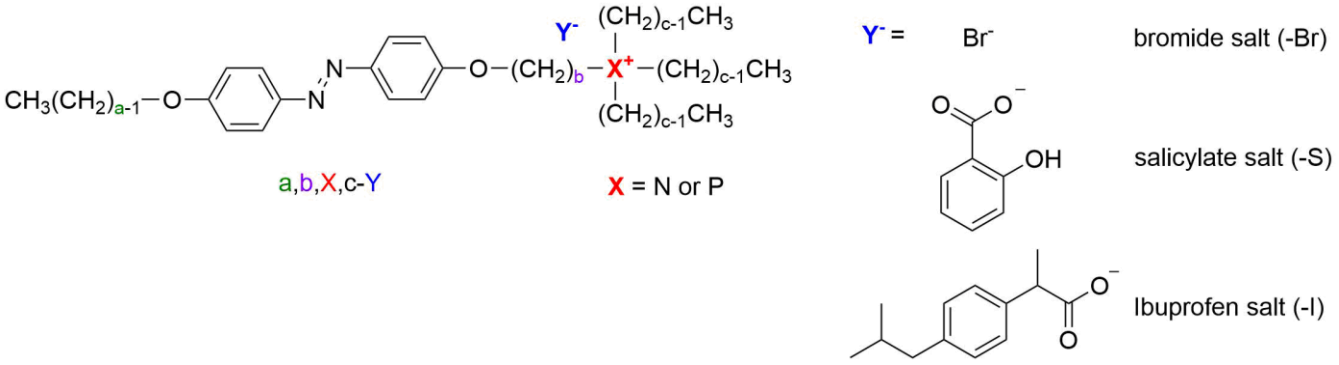

Scheme S1. Chemical structure of the photoswitchable salts with the cations a,b,X,c-Y with X = N or P and the anions Y = bromide, salicylate (S) or Ibuprofen (I).

In the **Supporting Information** the salts were coded for ease of presentation with a,b,X,c-Y, in which the number for a, b, c represents the length of the alkyl chains. For ammonium salts X = N and for phosphonium salts X = P was used. The corresponding anion was indicated for bromide salts with Y = -Br, for salicylate salts with Y = -S and for Ibuprofen salts with Y = -I.

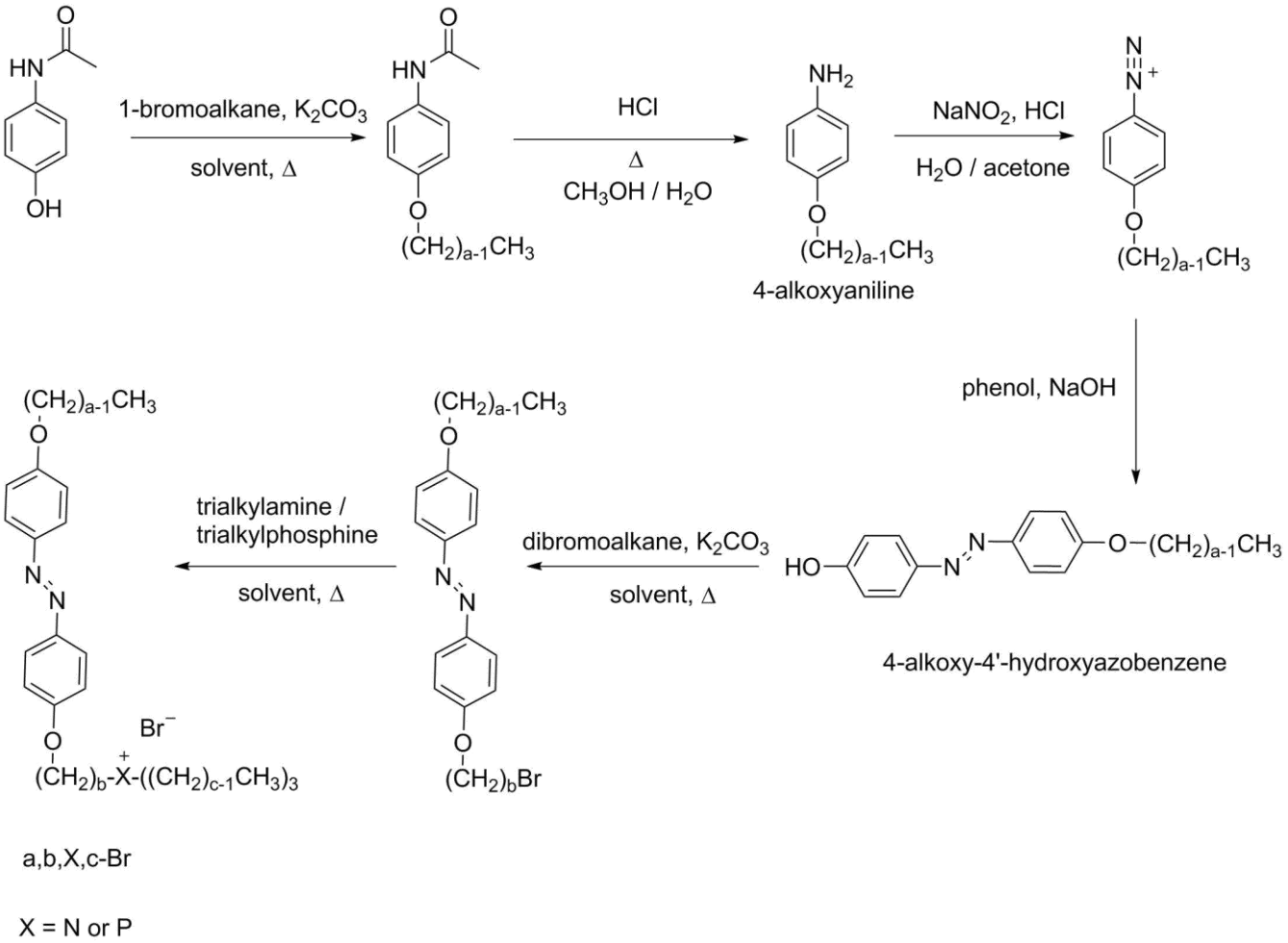

Scheme S2: Synthetic routes of the photoswitchable counterions a,b,X,c-Br. The strategy was adapted from Ishiba et al.[14]

Synthesis of 4-hexyloxyaniline

A suspension of 4-acetoamidophenol (30.2 g, 200 mmol), 1-bromohexane (42.9 g, 260 mmol) and potassium carbonate (71.9 g, 520 mmol) in acetone (300 mL) was heated under reflux for 18 h. 600 mL water was added and the colorless solid was filtered and dried. Excessive 1-bromohexane was removed by washing with hexane. The filtrated solid was dissolved in 300 mL mixed solvent of methanol and 35% hydrochloric acid (6:4). After 18 h reflux, 600 mL water was added and neutralized by sodium hydroxide. Extraction was done by 6 x 100 mL ethyl acetate and the organic layer was dried over anhydrous sodium sulfate. After removing of sodium sulfate by filtration and drying under reduced pressure an orange brown solid was obtained.
Yield: 27.64 g (72%). ^{1}H-NMR ($CDCl_3$, δ [ppm], *J* [Hz]): 6.78 – 6.72 (m, 2H), 6.70 – 6.63 (m, 2H), 3.88 (t, *J* = 6.6, 2H), 1.78 – 1.69 (m, 2H), 1.49 – 1.40 (m, 2H), 1.38 – 1.29 (m, 4H), 0.93 – 0.87 (m, 3H).

Synthesis of 4-hexyloxy-4'-hydroxyazobenzene

4-hexyloxyaniline (16.55 g, 86 mmol) was dissolved in 600 mL water and acetone (1:2) with 22 mL 35% hydrochloric acid (264 mmol). Below 5 °C a solution of sodium nitrite (7.62 g, 110.4 mmol) in 30 mL water was added and a solution of phenol (10.4 g, 110.6 mmol) and sodium hydroxide (10.54 g, 264 mmol) in 100 mL water was added. The mixture was stirred for 4 h in an ice bath to keep the reaction temperature below 10 °C and stirred overnight at room temperature. The solution was neutralized using 6 N hydrochloric acid and the suspended solid was filtered. After recrystallization in 780 mL solvent of water and ethanol (1:2) dark red crystals were obtained.
Yield: 11.1 g (43%). ^{1}H-NMR ($CDCl_3$, δ [ppm], *J* [Hz]): 7.95 – 7.78 (m, 4H), 7.05 – 6.89 (m, 4H), 4.02 (t, *J* = 6.6, 2H), 1.87 – 1.76 (m, 2H), 1.55 – 1.43 (m, 2H), 1.39 – 1.31 (m, 4H), 0.95 – 0.89 (m, 3H).

Synthesis of 4-hexyloxy-4'-(4-bromobutyloxy)-azobenzene

A suspension of 4-hexyloxy-4'-hydroxyazobenzene (9.49 g; 31.8 mmol), 1,4-dibromobutane (35.5 g, 160 mmol) and potassium carbonate (13.8 g, 99.9 mmol) in 300 mL acetone was heated under reflux for 12 h. After evaporation of solvent, 300 mL water was added to the mixture. The suspended solid was filtered, dried and recrystallized in mixed solvent of chloroform and ethyl acetate (2:1) to give a yellow solid. Yield: 11.5 g (83%). ^{1}H-NMR ($CDCl_3$, δ [ppm], *J* [Hz]): 7.77 – 7.94 (m, 4H), 6.93 – 7.04 (m, 4H), 4.08 (t, *J* = 6.0, 2H), 4.03 (t, *J* = 6.6, 2H), 3.51 (t, *J* = 6.4, 2H), 2.04 – 2.16 (m, 2H), 1.93 – 2.04 (m, 2H), 1.82 (quin, *J* = 6.5, 2H), 1.42– 1.56 (m, 2H), 1.28 – 1.42 (m, 4H), 0.92 (t, *J* = 7.1, 3H).

*Synthesis of the tripropylammonium bromide salt (**Figure 1A**)*

A suspension of 4-hexyloxy-4'-(4-bromobutyloxy)-azobenzene (3.80, 8.77 mmol) and tripropylamine (3.77 g, 26.31 mmol) in acetonitrile (40 mL) was refluxed for 7 d. After evaporation of the solvent, the crude product was washed with diethyl ether and after drying a yellow crystalline solid was obtained. Yield: 3.47 g (69%). ^{1}H-NMR (DMSO-d_6, δ [ppm], *J* [Hz]): 8.13 – 7.53 (m, 4H), 7.39 – 6.79 (m, 4H), 4.20 – 4.10 (m, 2H), 4.06 (t, *J* = 5.3, 2H), 3.30 – 3.22 (m, 2H), 3.22 – 3.06 (m, 6H), 1.90 – 1.77 (m, 4H), 1.77 – 1.71 (m, 2H), 1.71 – 1.52 (m, 6H), 1.50 – 1.37 (m, 2H), 1.37 – 1.25 (m, 4H), 0.90 (t, *J* = 7.2, 9H), 0.88 (t, *J* = 7.1, 3H). ^{13}C-NMR: 161.0, 160.6, 146.2, 146.0, 124.1, 124.1, 115.0, 114.9, 67.9, 66.9, 59.3, 57.4, 31.0, 28.5, 25.3, 25.1, 22.0, 17.9, 14.8, 13.9, 10.5.

MS m/z calcd for $C_{31}H_{50}N_3O_2^+$, 496.4; found 496.4

m.p.: 134 °C (DSC)

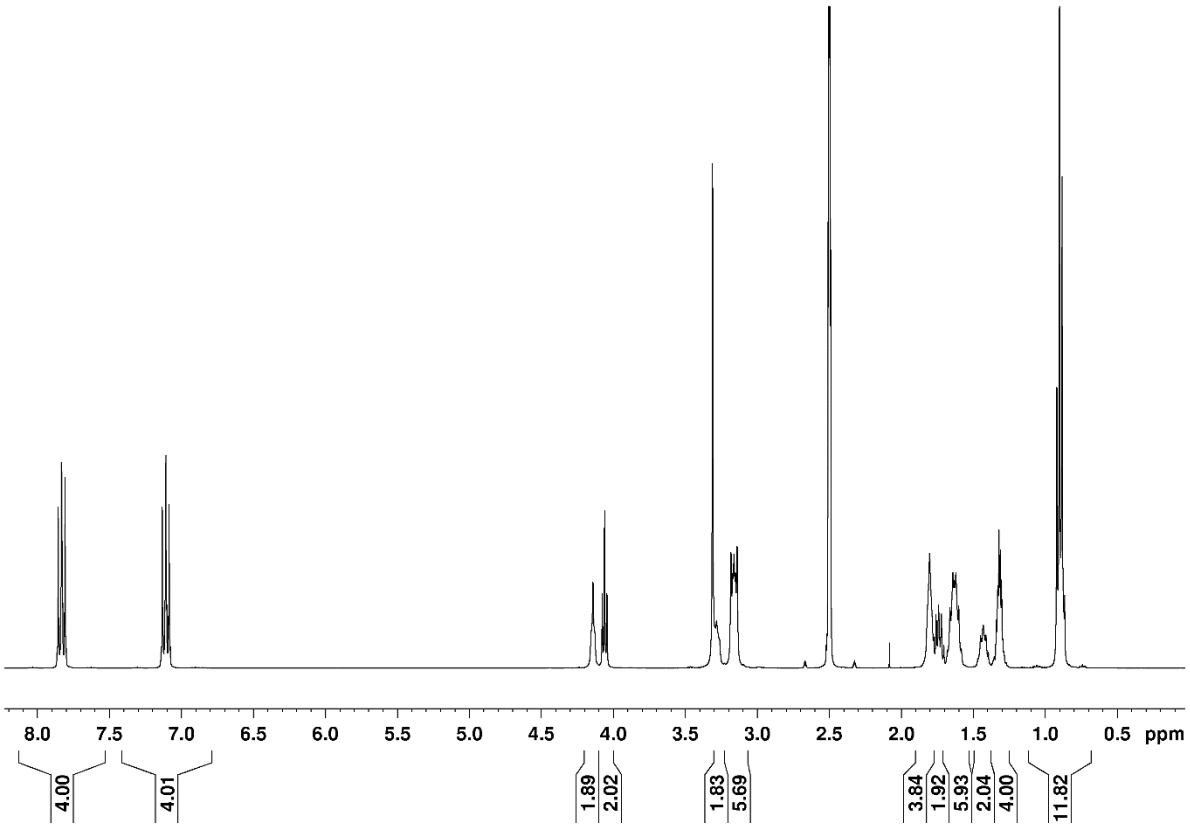

Figure S1. ^{1}H-NMR spectrum of tripropylammonium bromide salt (**Figure 1A**) in DMSO-d_6.

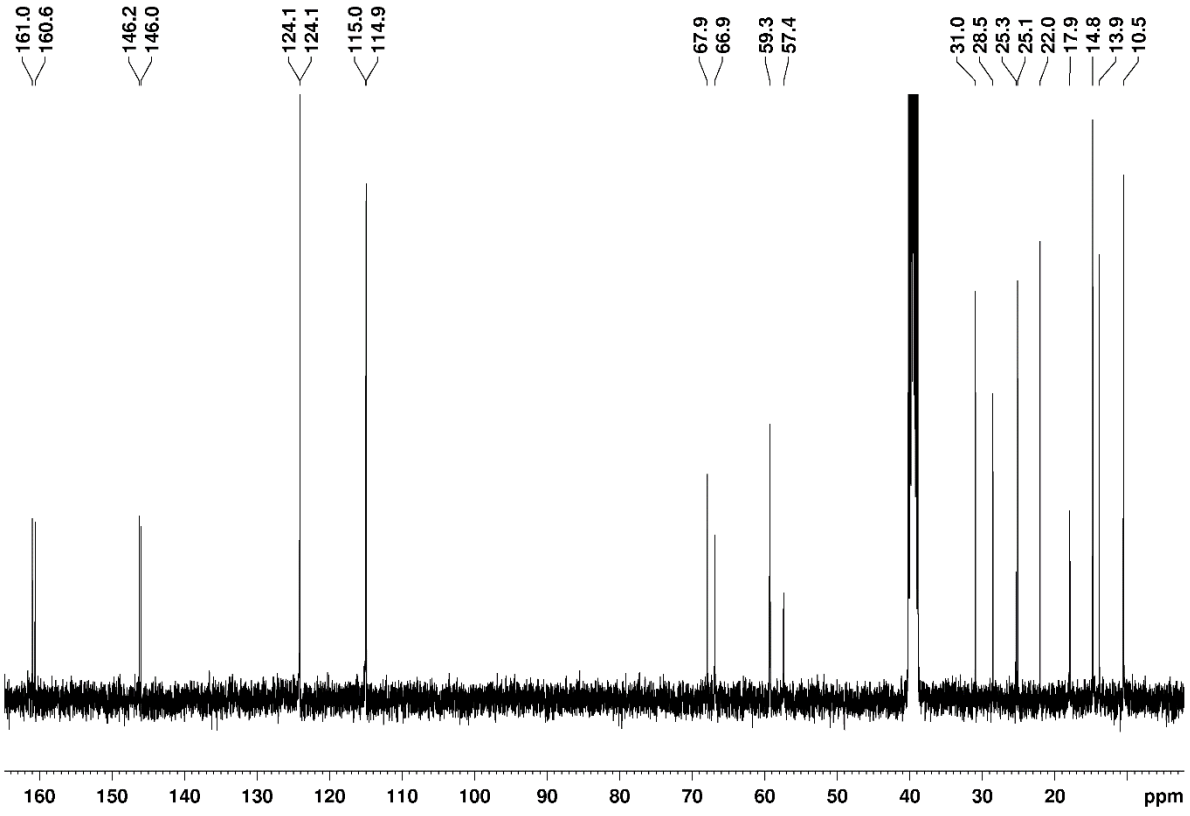

Figure S2. ^{13}C-NMR spectrum of tripropylammonium bromide salt (**Figure 1A**) in DMSO-d_6.

*Synthesis of trimethylphosphonium bromide salt (**Figure 1A**)*

A suspension of 4-hexyloxy-4'-(4-bromobutyloxy)-azobenzene (1.70 g, 3.93 mmol) and trimethylphosphine (0.45 g, 5.91 mmol) in acetonitrile (20 mL) was heated at 40 °C for 120 h. After evaporation of the solvent, the crude product was washed with diethyl ether and after drying a yellow crystalline solid was obtained. Yield: 1.43 g (71%). ^{1}H-NMR (DMSO-d_6, δ [ppm], *J* [Hz]): 8.07 – 7.57 (m, 4H), 7.35 – 6.80 (m, 4H), 4.13 (t, J = 6.2, 2H), 4.06 (t, J = 6.4, 2H), 2.35 – 2.23 (m, 2H), 1.95 – 1.79 (m, 2H), 1.85 (d, J = 14.8, 9H), 1.78 – 4.63 (m, 4H), 1.49 – 1.38 (m, 2H), 1.38 – 1.25 (m, 4H). ^{13}C-NMR: 160.6, 160.7, 146.2, 146.0, 124.1, 124.1, 115.0, 114.9, 67.9, 67.0, 30.9, 29.4 (d, J = 16.3), 28.5, 25.1, 22.0, 22.0 (d, J = 52.4), 17.6 (d, J = 3.8), 13.9, 7.2 (d, J = 53.9).

MS m/z calcd for $C_{25}H_{38}N_2O_2P^+$, 429.3; found 492.3

m.p.: 87 °C under degradation (DSC)

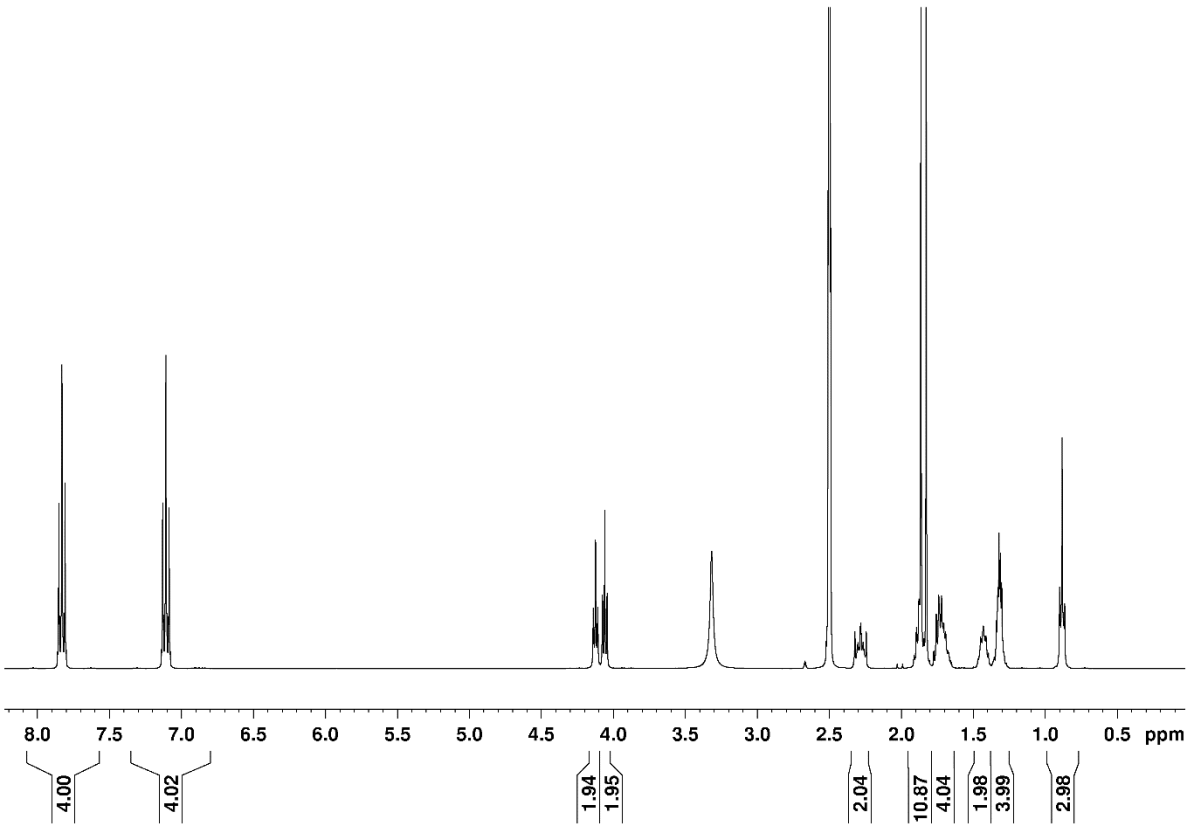

Figure S3. ^{1}H-NMR spectrum of trimethylphosphonium bromide salt (**Figure 1A**) in DMSO-d_6.

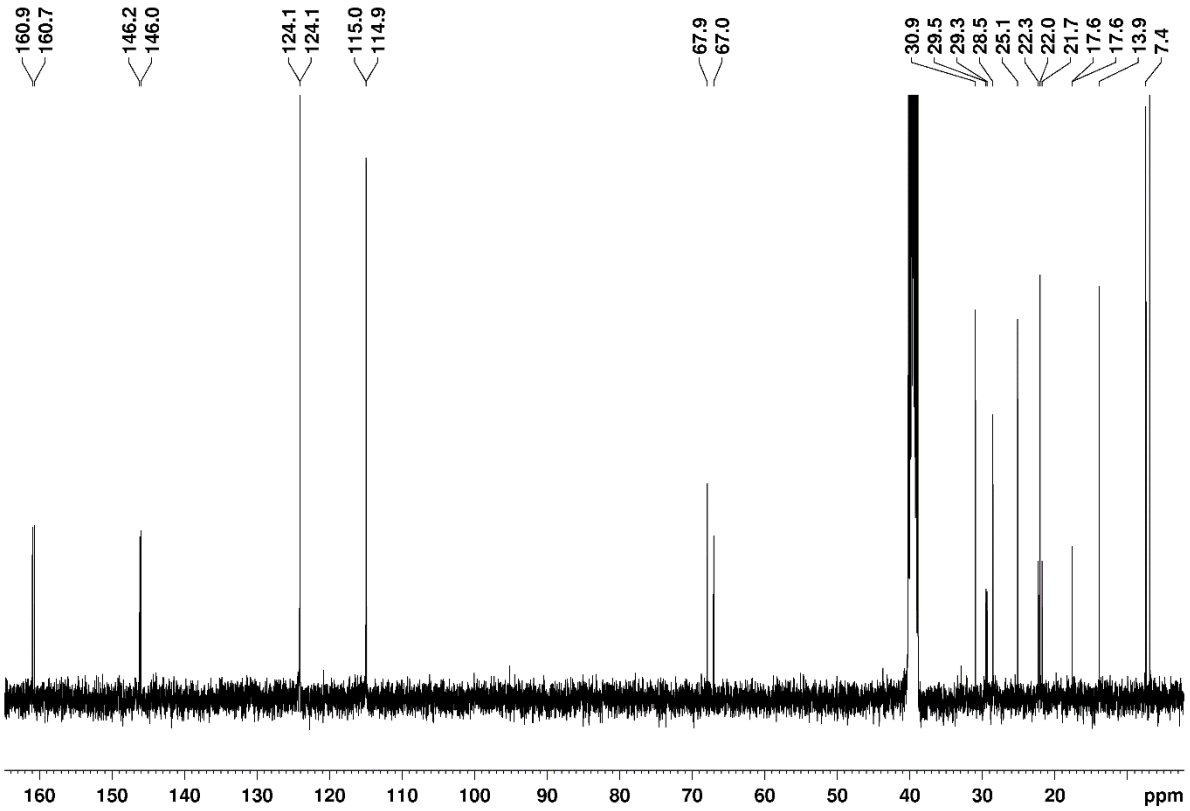

Figure S4. ^{13}C-NMR spectrum of trimethylphosphonium bromide salt (**Figure 1A**) in DMSO-d_6.

*Preparation of the of tripropylammonium salicylate salt (**Figure 1A**)*

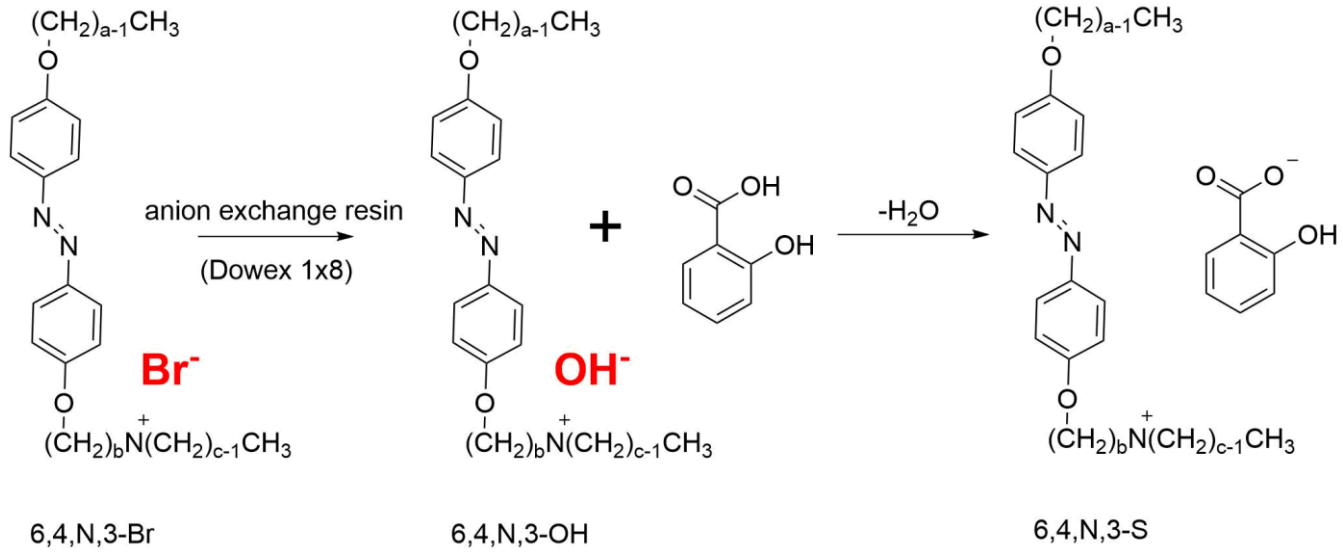

Scheme S3. Preparation of salicylate salts with photoswitchable counterions.

0.52 g 6,4,N,3-Br dissolved in 1000 mL MeOH was slowly eluted (10 drops/ min) through a column with anion exchange resin (Dowex 1 x 8) in hydroxide form. Complete anion exchange was controlled by addition of nitric acid and silver nitrate. After the eluate was reduced to approximately 50 mL volume *in vacuo*, a precipitation was observed, which was removed by centrifugation (4000 rpm, 10 min). The content of the clear solution was measured by quantitative ^{1}H NMR spectroscopy using the internal standard maleic acid (Fluka, Schweiz). 50 µL sample was mixed with 550 µL DMSO-d_6 and 1.398 mg maleic acid. The ^{1}H measurement was performed using the parameters in **Tab S1**. The integrals of the ^{1}H resonances of maleic acid — between the ^{13}C satellites (δ = approx. 6.1 – 6.4 ppm) and the aromatic ^{1}H signals of 6,4,N,3-OH (δ = 8 – 7 ppm) — were used to assess the content with Eq. (1):

$$m_{sample} = \frac{I_{sample}}{I_{ref}} * \frac{N_{ref}}{N_{sample}} * \frac{M_{sample}}{M_{ref}} * m_{ref} * \frac{P_{ref}}{P_{sample}} \qquad \text{[Eq. (1)]}$$

(m = mass in mg, I = integrated area, P = purity, N = number of protons under the signal, M = molecular weight)

Table S1. Parameter for quantitative ^{1}H-NMR spectroscopy

acquisition	
probe head	BBO BB-1H/D/19F Z-GRD
Pulse program	zg30
Data points	64k
solvent	DMSO-d_6
temperature	300 K
rotation	off
Number of scans	64
Spectral width	20.55
O1	6.175
Acquisition time	3.984 s
Digital resolution	0.251 Hz/Pkt.
Relaxation delay D1	60 s
processing	
Data points	64k
Window function	exponential
LB factor	0.30 Hz

Result: 0.839 mg / 50 µL.

21.82 mg salicylic acid was dissolved in 4 mL methanol and 4837 µL 6,4,N,3-OH solution was added under stirring until a clear yellow solution was obtained. After slowly evaporation of the solvent a yellow, crystalline solid crystallized, which was dried at room temperature 24 h under reduced pressure.

^{1}H-NMR (DMSO-d_6, δ [ppm], *J* [Hz]): 7.91 – 7.75 (m, 4H), 7.62 (dd, *J* = 7.6, *J* = 1.7, 1H), 7.20 – 7.00 (m, 5H), 6.64 – 6.48 (m, 2H), 4.20 – 4.10 (m, 2H), 4.07 (t, *J* = 6.5, 2H), 3.28 – 3.24 (m, 4H), 3.20 – 3.08 (m, 6H), 1.86 – 1.77 (m, 4H), 1.77 – 1.69 (m, 2H), 1.69 – 1.55 (m, 6H), 1.49 – 1.38 (m, 2H), 1.38 – 1.26 (m, 4H), 0.90 (t, *J* = 7.2, 9H), 0.88 (t, *J* = 5.6, 3H).

^{13}C-NMR: 171.1, 163.0, 161.0, 160.6, 146.3, 146.0, 131.6, 129.9, 124.1, 124.1, 119.9, 115.9, 115.9, 115.0, 115.0, 67.9, 66.9, 59.3, 57.4, 30.6, 28.6, 25.3, 25.1, 22.0, 17.9, 14.8, 13.9, 10.5.

HRMS-ESI positive mode: m/z calcd for $C_{31}H_{50}N_3O_2^+$,496.39; found 496.39

HRMS-ESI negative mode: m/z calcd for $C_7H_5O_3^-$,137.02; found 137.02

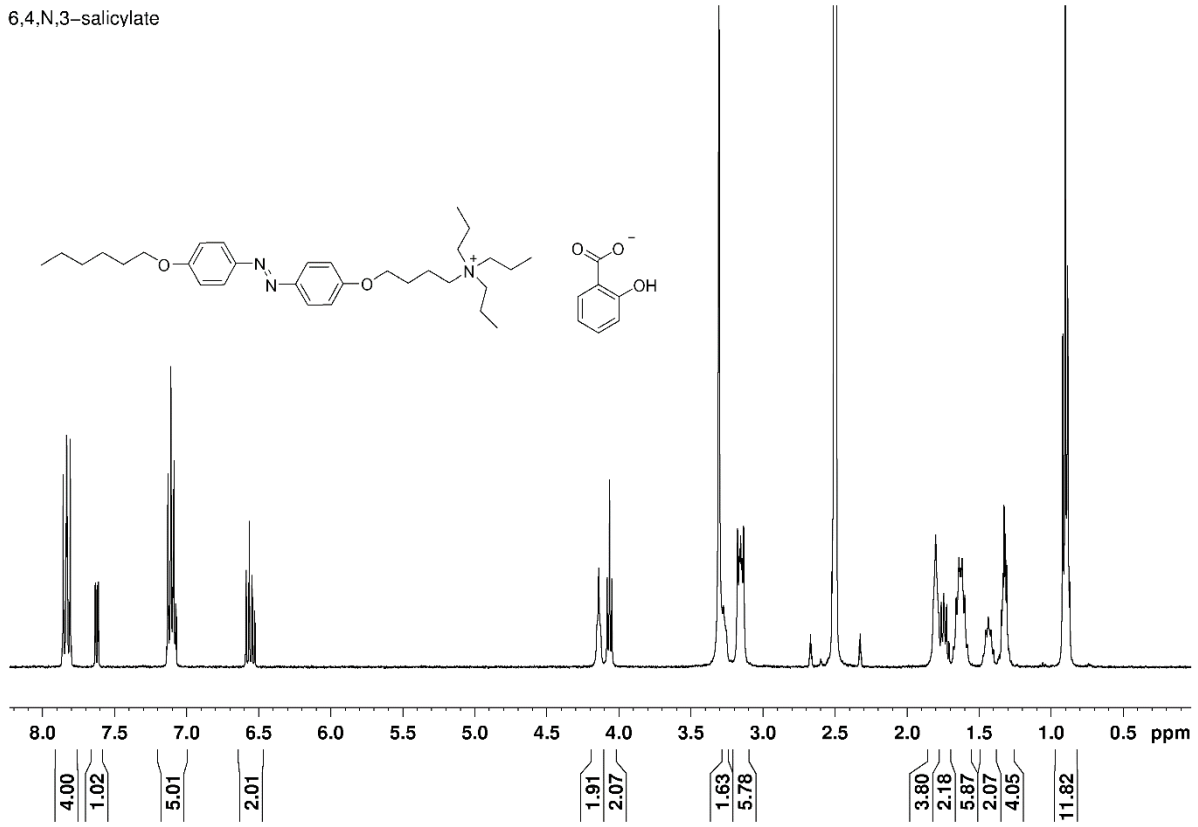

Figure S5. ^{1}H-NMR spectrum of tripropylammonium salicylate salt (**Figure 1A**) in DMSO-d_6.

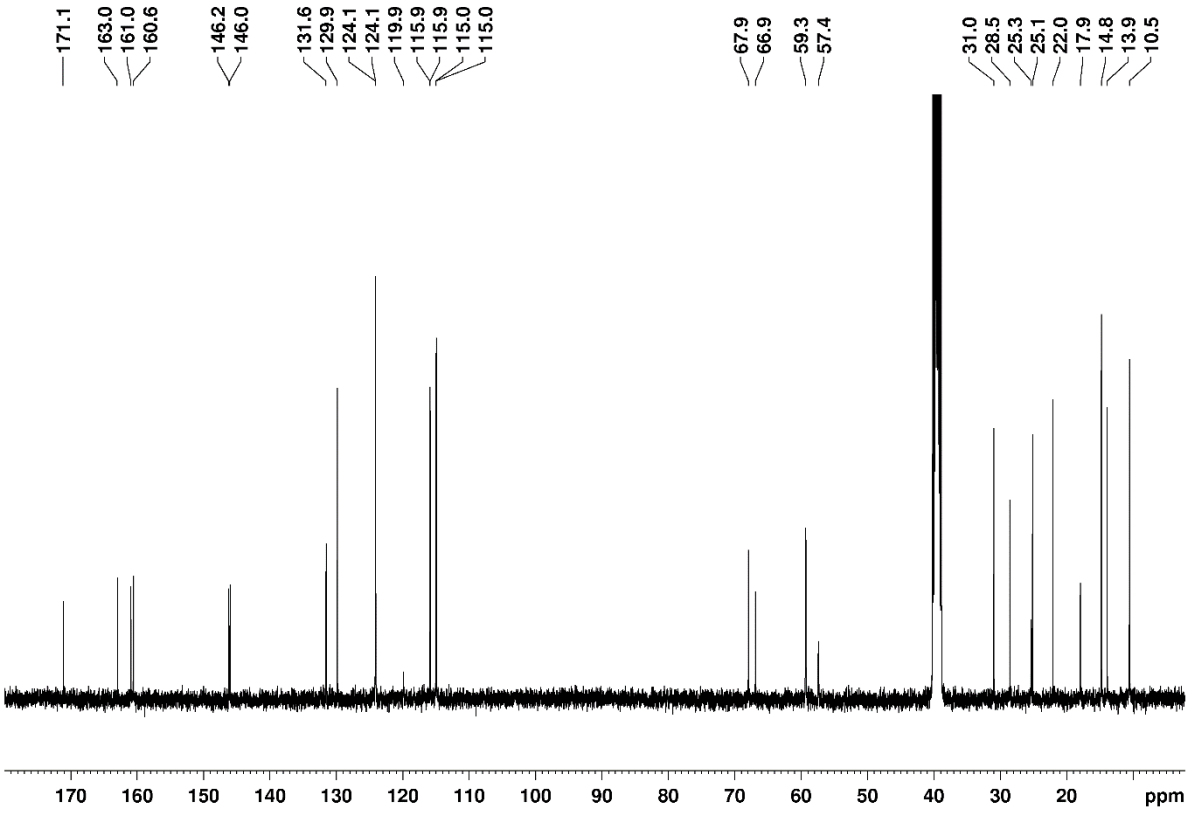

Figure S6. ^{13}C-NMR spectrum of the tripropylammonium salicylate salt (**Figure 1A**) in DMSO-d_6.

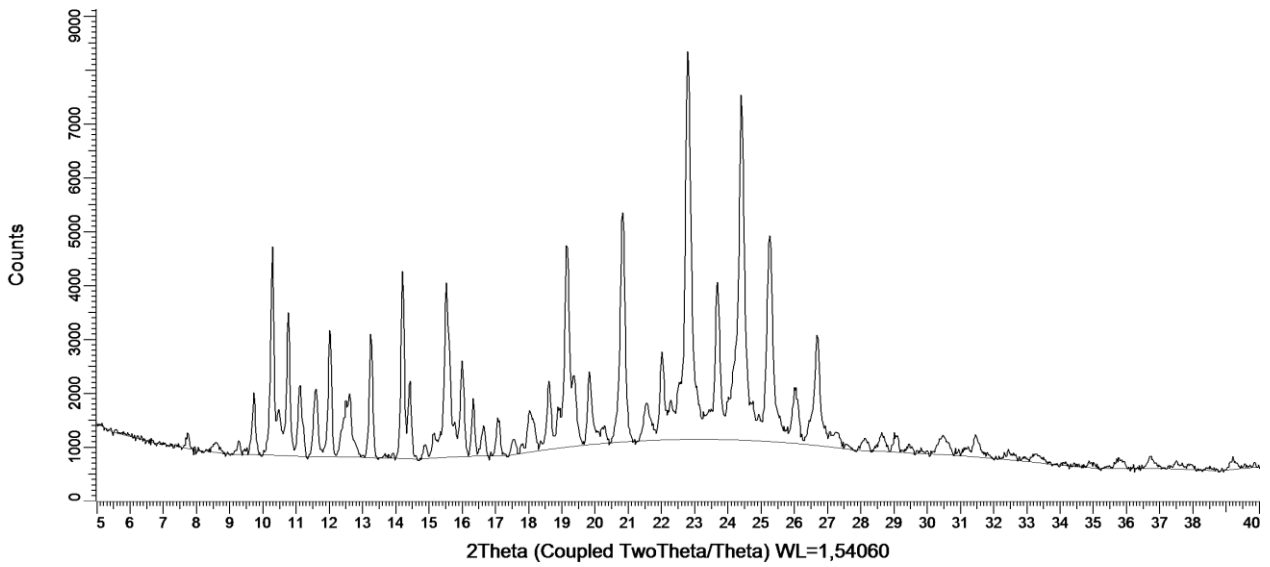

Figure S7. Powder XRD diffractogram of the crystalline tripropylammonium salicylate salt (**Figure 1A**) (not irradiated) at room temperature.

*Preparation of the P+ ibuprofen (trimethylphosphonium ibuprofenat salt (**Figure 1A**)*

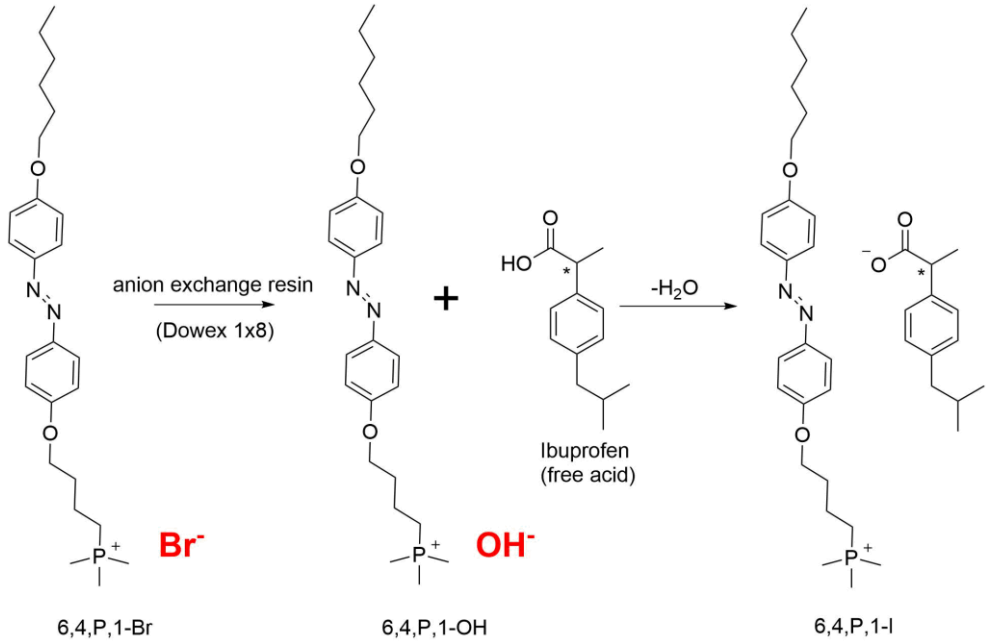

Scheme S4. Preparation of the photoswitchable Ibuprofen salt.

The anion exchange, quantitative ^{1}H NMR spectroscopy and salt preparation was done as described before. The product crystallized in dark by slowly solvent evaporation at room temperature and standard pressure over 5 days. The salt was dried 24 h under reduced pressure at room temperature. The ratio of the counterion to API was 1:1 determined by ^{1}H NMR spectroscopy, using the area under the signals of the aromatic ^{1}H signal at 7.9 – 7.75 ppm and 1.20 – 1.12 ppm for Ibuprofen.

^{1}H-NMR (DMSO-d_6, δ [ppm], *J* [Hz]): 7.90 – 7.75 (m, 4H), 7.18 – 7.03 (m, 6H), 6.98 – 6.88 (m, 2H), 4.12 (t, *J* = 6.1, 2H), 4.06 (t, *J* = 6.6, 2H), 3.10 (q, *J* = 7.1, 1H), 2.35 (d, *J* = 7.1, 2 H), 2.32 – 2.20 (m, 2H), 1.93 – 1.79 (m, 2H), 1.83 (d, *J* = 14.8, 9H), 1.85 – 1.63 (m, 5H), 1.49 – 1.38 (m, 2H), 1.37 – 1.28 (m, 4H), 1.16 (d, *J* = 7.1, 3H), 0.92 – 0.86 (m, 3H), 0.85 (d, *J* = 6.6, 6H).

^{13}C-NMR: 174.9, 161.0, 160.7, 146.2, 146.0, 144.1, 136.9, 127.8, 127.2, 124.1, 124.1, 115.0, 114.9, 67.9, 67.0, 49.3, 44.4, 31.0, 29.7, 29.4 (d, *J* = 16.4), 28.5, 25.1, 22.2, 22.0, 22.0 (d, *J* = 52.4), 20.5, 17.6 (d, *J* = 3.7), 13.9, 7.1 (d, *J* = 53.9).

HRMS-ESI positive mode: m/z calcd for $C_{25}H_{38}N_2O_2P^+$, 429.27; found 429.27

HRMS-ESI negative mode: m/z calcd for $C_{13}H_{17}O_2^-$, 205.12; found 205.12

Elemental analysis (%) calcd for $C_{38}H_{55}N_2O_4P$ + 3 H_2O: C, 66.25; H, 8.93; N, 4.07. Found: C, 66.42; H, 8.64; N, 3.98.

m.p.: 107 °C (DSC)

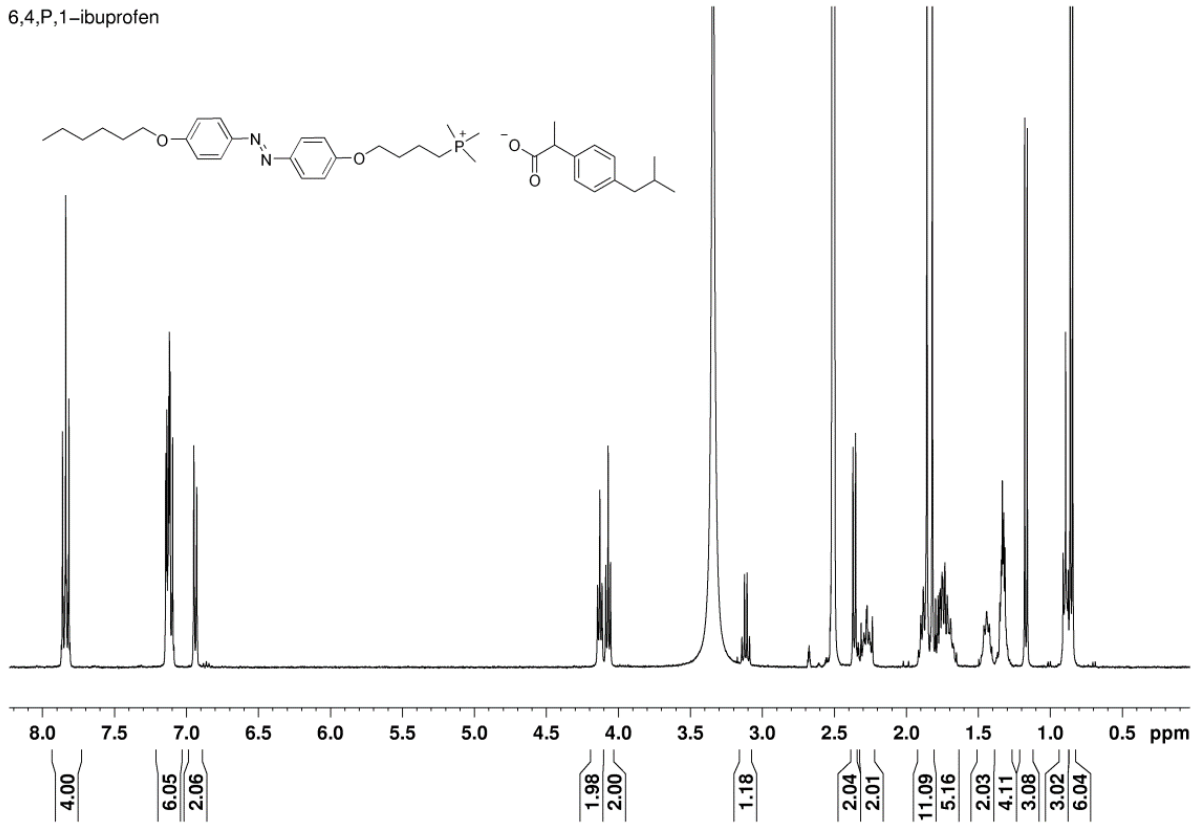

Figure S8. ^{1}H-NMR spectrum of P^{+} ibuprofen (trimethylphosphonium ibuprofenat salt (**Figure 1A**) in DMSO-d_6.

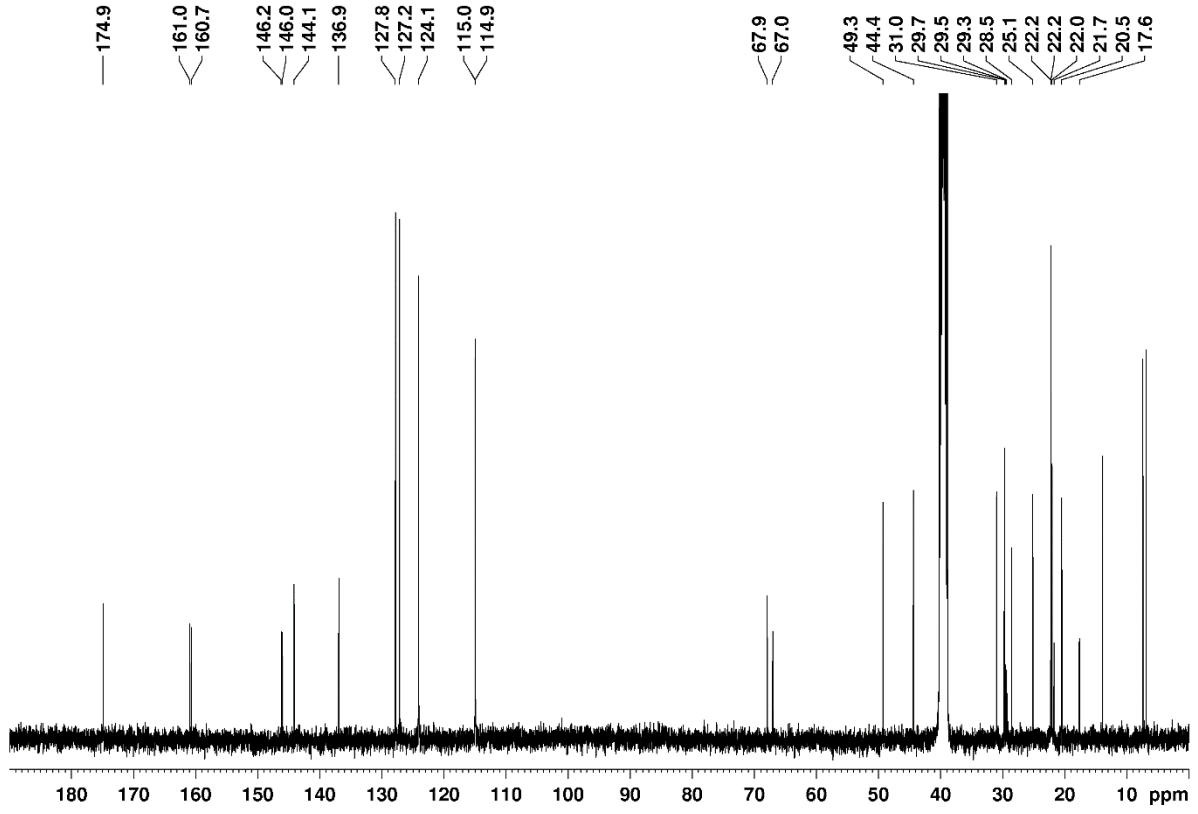

Figure S9. ^{13}C-NMR spectrum of P^{+} ibuprofen in DMSO-d_6.

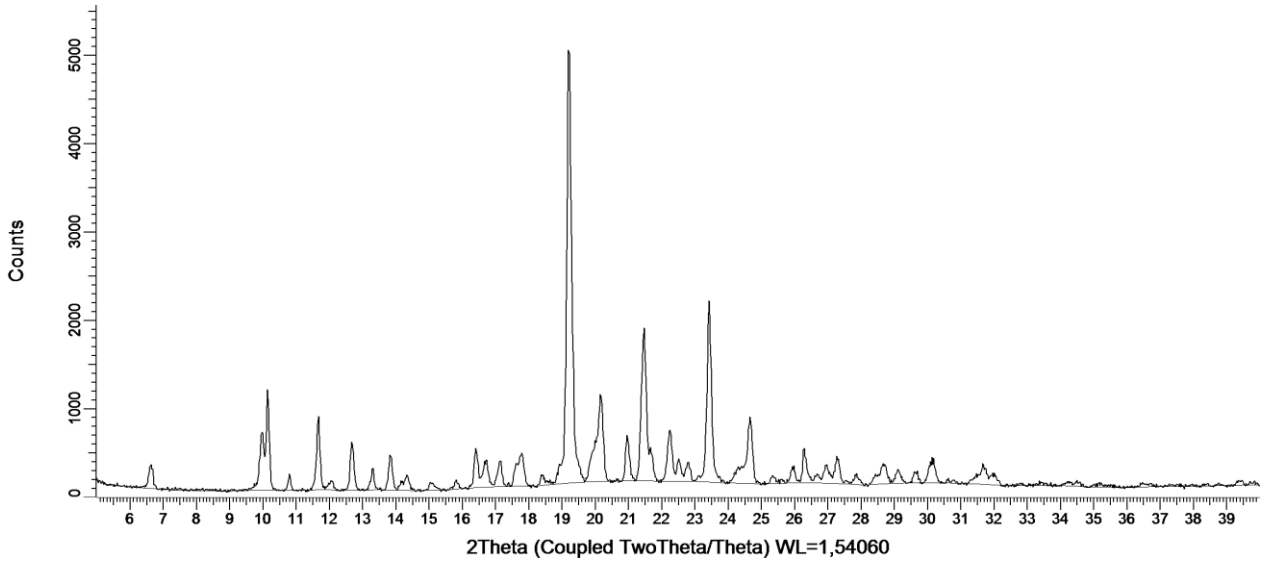

Figure S10. Powder X-ray powder diffractogram of the crystalline photoswitchable Ibuprofen salt P^+ ibuprofen (dark = not irradiated) at room temperature.

Results and Discussion

Cis-to-*trans* ratio by HPLC

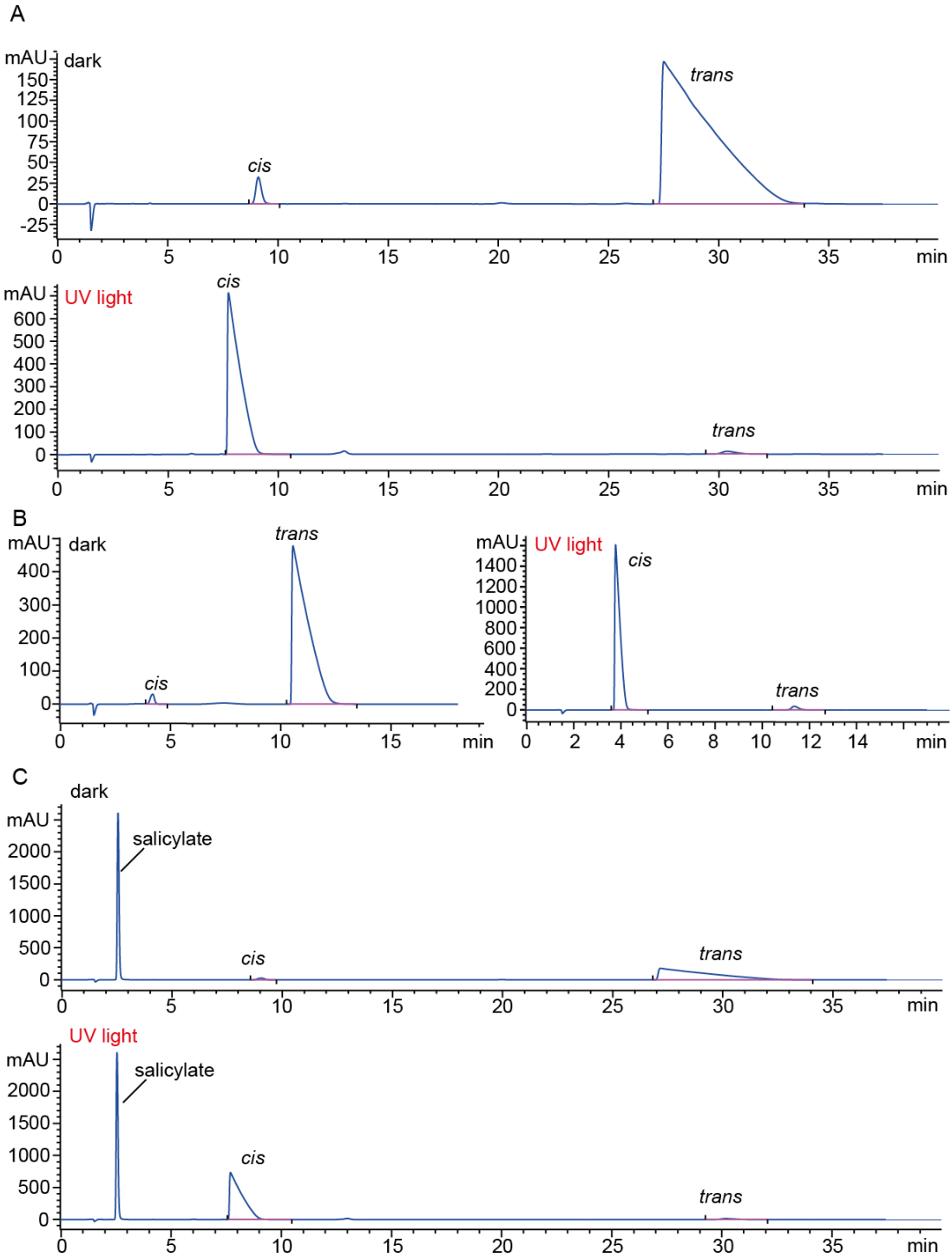

Figure S11. HPLC chromatograms of (A) tripropylammonium bromide salt (**Figure 1A**), (B) trimethylphosphonium bromide salt (**Figure 1A**) and (C) the tripropylammonium salicylate salt in dark and after UV light exposure. The *cis* and *trans* form of the azobenzene counterions were separated and the area under the peaks was used to calculate the *cis*-to-*trans* ratio.

Aggregate state of the ibuprofen azobenzene salts

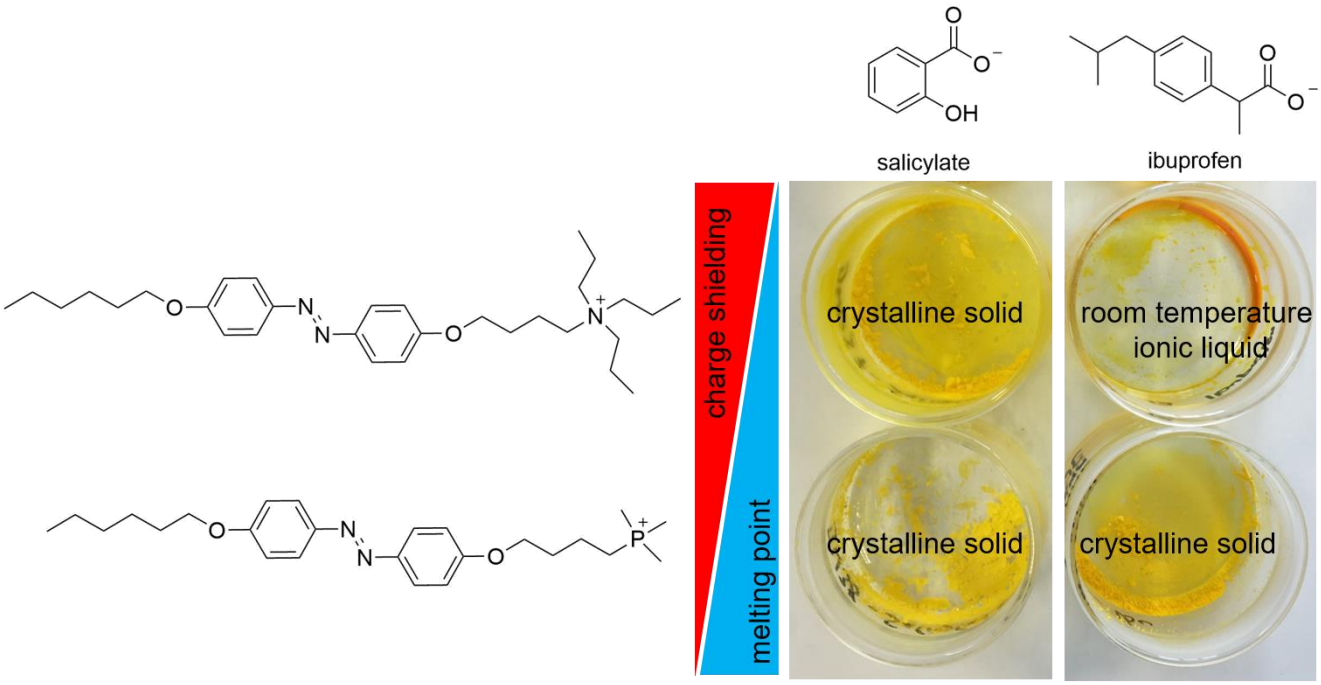

Figure S12. Overview of the photoswitchable pharmaceutical salts with salicylate or Ibuprofen, respectively.

The bigger size of Ibuprofen compared to salicylate potentially hindered the crystallization with the ammonium counterion resulting in a room temperature ionic liquid. Reduced shielding of the positive charge by using methyl instead of propyl chains and an increased size of the polar head group (from ammonium to phosphonium) resulted in a crystalline solid with Ibuprofen at room temperature.

Dynamic scanning calorimetry (DSC)

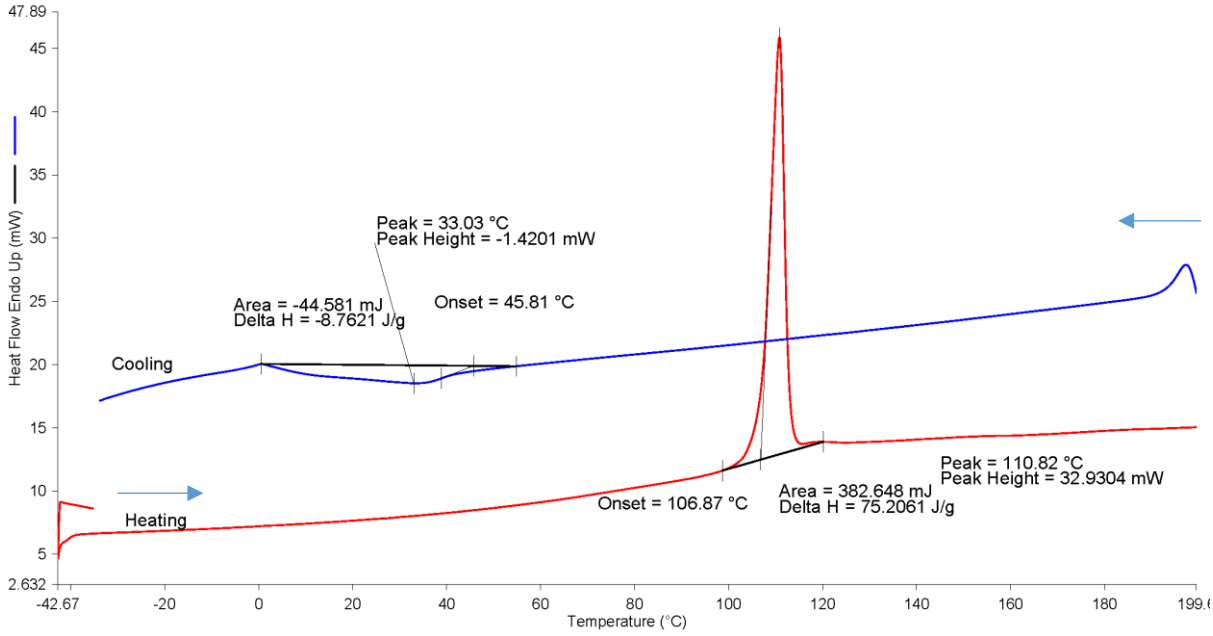

Figure S13. DSC thermogram of the trans-isomer of the P+-Ibuprofen crystalline solid powder (dark) with a heating rate of 20 °C/min from -50 to 200 °C followed by cooling with a rate of 50 °C/min from 200 to -50 °C. The melting point was 107 °C and no crystallization was observed during this rapid cooling cycle possibly reflecting a slow nucleation process.

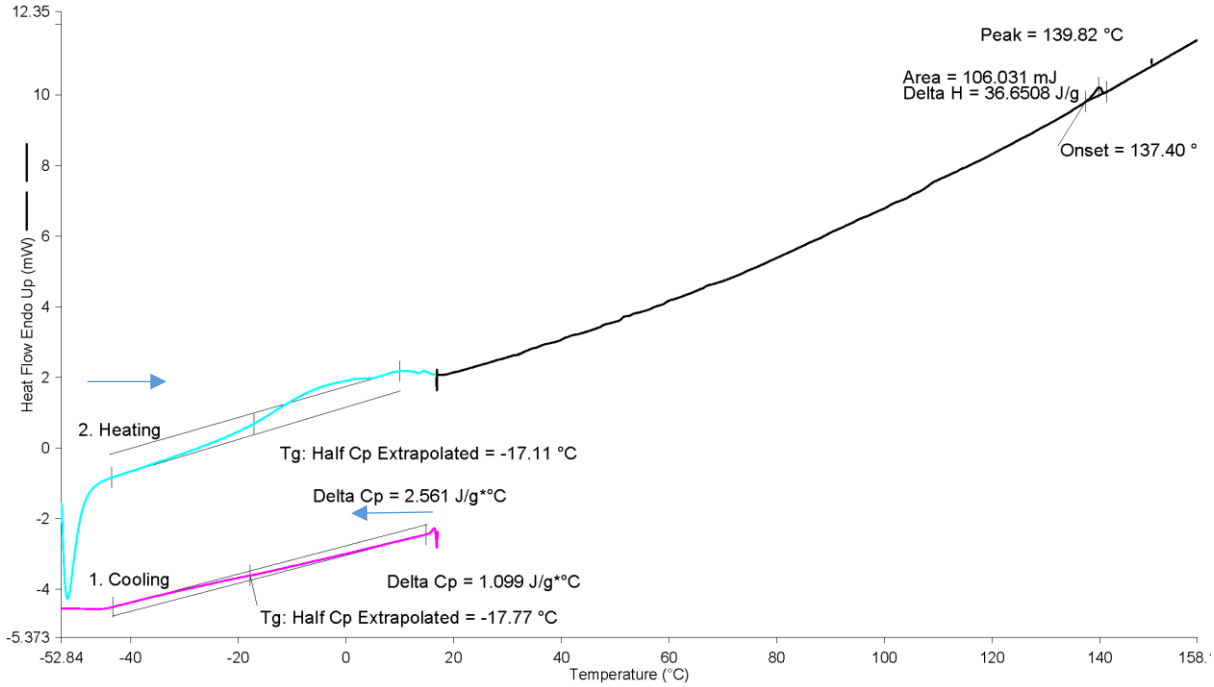

Figure S14. DSC thermogram of the amorphous room-temperature ionic liquid after UV-light irradiation of the powdered sample of P+-Ibuprofen with a cooling rate of 5 °C/min from 20 to -50 °C followed by heating with a rate of 5 °C/min from -50 to 20 °C. Between 20 °C and 160 °C the heating rate was reduced from 5 °C/min to 0.2 °C/min to catch slow recrystallization processes due the thermally induced *cis*-to-*trans* isomerization. Despite the slow heating rate no recrystallization was observed, indicating that the kinetic of nucleation and recrystallization is very slow under this conditions possibly reflecting due the high viscosity of the liquid phase and/or the size of the counterion and Ibuprofen. The endothermic peak at 137 °C could indicate a phase transition from a mesophase to an isotropic liquid.

Wide- and small-angle X-ray scattering

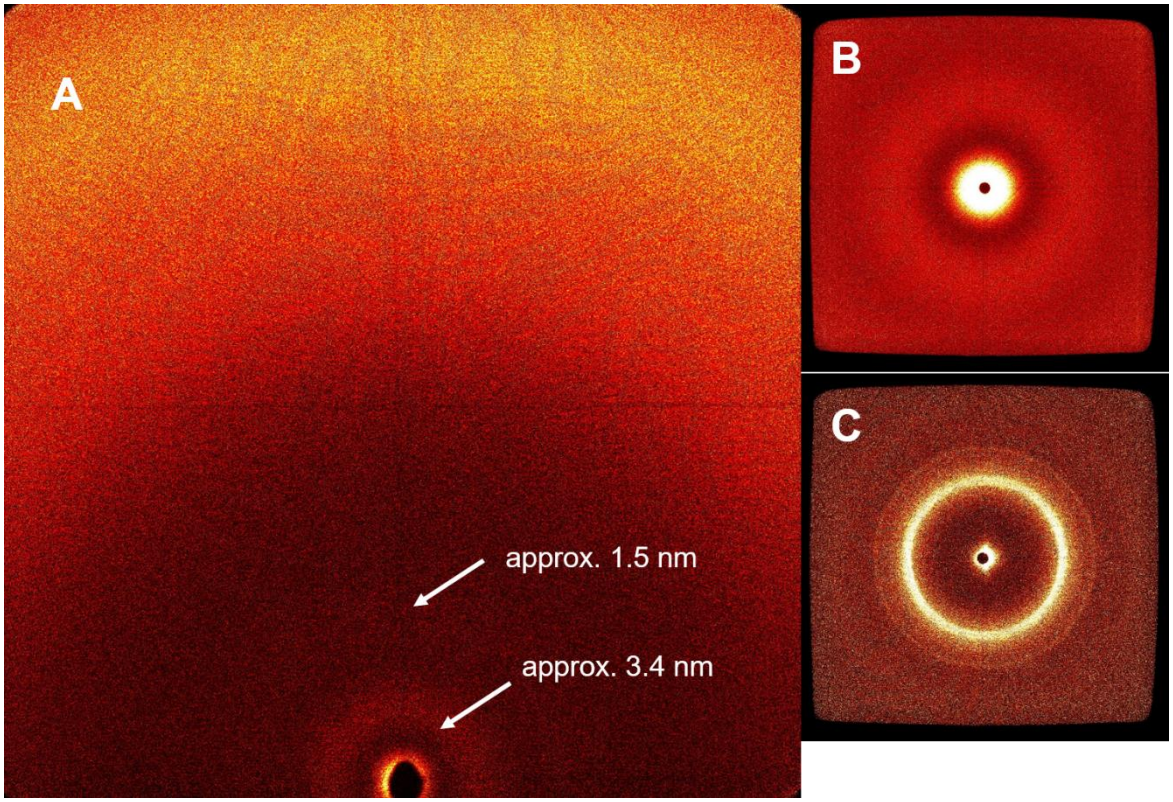

Figure S15. Hydrogel characterization by WAXS and SAXS measurements. (A) WAXS XRS: A halo at wide angles (water); a weak signal at 3.4 nm and a much weaker signal at 1.5 nm were observed. (B) SAXS pattern with a signal at 3.4 nm and strong intensity about the beam stop pointing to strong scattering of nano-morphology of the gel sample. (C) After UV light irradiation sharper signals and reduced scattering around the beam stop were observed.

The gel structure was studied by wide- and small-angle X-ray scattering (WAXS/SAXS). The correlation length (ξ/nm), which indicates the degree of order in the structure, was calculated through the Scherrer formula ($\xi = \lambda/(\Delta\theta\cos\theta)$, where λ is the wavelength of X-rays 0.154 nm; $\Delta\theta$ the is full-width-at-half-maximum (FWHM) of the reflection in radians; θ is the reflection position in degree.[15-16] In dark (99% *trans*) a broad low intense signal at 3.4 nm (correlation length of 3.5 nm (Scherrer formula)) and a much weaker signal at 1.5 nm was observed with WAXS indicating a double layer arrangement with antiparallel intercalated ion pairs with a length of 2.8-2.9 nm separated of a water layer of about 0.5 nm (about 2-3 water molecules). After 75 min irradiation with UV light most of the water (about 70%) was squeezed out and two sharp reflexed were observed indicating the formation of a periodic, ordered structure (C). This process was reversible shown by time-dependent SAXS measurements (**Figure S16**) and could also be followed visibly by a reuptake of the water and the color change from intense red (*cis*) to yellow (*trans*).

Time-dependent SAXS measurements

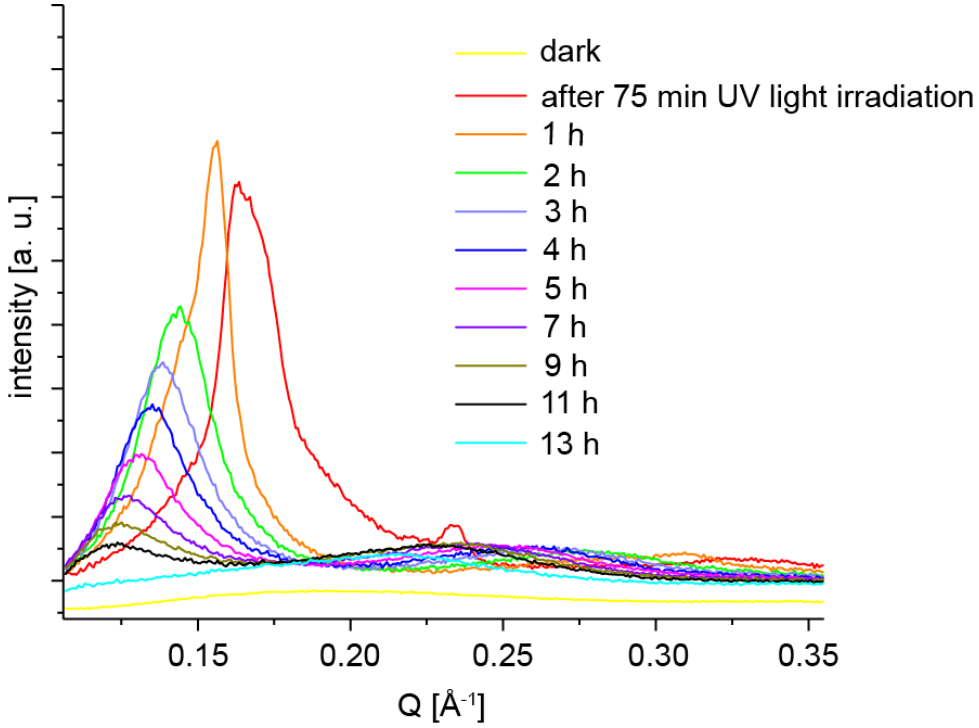

Figure S16. Q [Å^{-1}] plotted against the intensity of the SAXS measurements before and after UV light exposure at different time points.

UV light exposure (75 min) pushed out a large portion of the water of the hydrogel during the photochemical process (approx. 70%) and a periodic structure was formed with sharper signals in the SAXS experiment (red pattern).The signal of the second diffraction pattern after irradiation (after 1 hour) was fitted with two Voigt functions. The rather sharp signal corresponds to a size of 4.0 nm with a correlation length of 69.0 nm (i.e. 16 repeating units); the broader shoulder to 4.2 nm with a correlation length of 17.2 nm (i.e. 4 repeating units). This broader shoulder reduced subsequently in intensity and shifts to smaller angles corresponding to 5.1 nm after 11 h; a further experiment started after 13 h revealed that the latter signal disappeared completely and only a broad signal remained with low intensity. This could be fitted with two Voigt functions with 2.86 nm (9.24 nm correlation length; 3.2 repeating units) and 3.62 nm (3.13 nm correlation length i.e. 0.86 repeating units). The latter was identical to the signal found for the original gel. The previously separated water was partially reabsorbed by recovering the hydrogel, although separated by an air bubble. The first signal at 2.86 nm was different from the original structure probably because the water uptake has not been finished within the 13 h of the experiment.

***Cis-trans* ratio of trimethylphosphonium ibuprofenate salt (P^+ ibuprofen)**

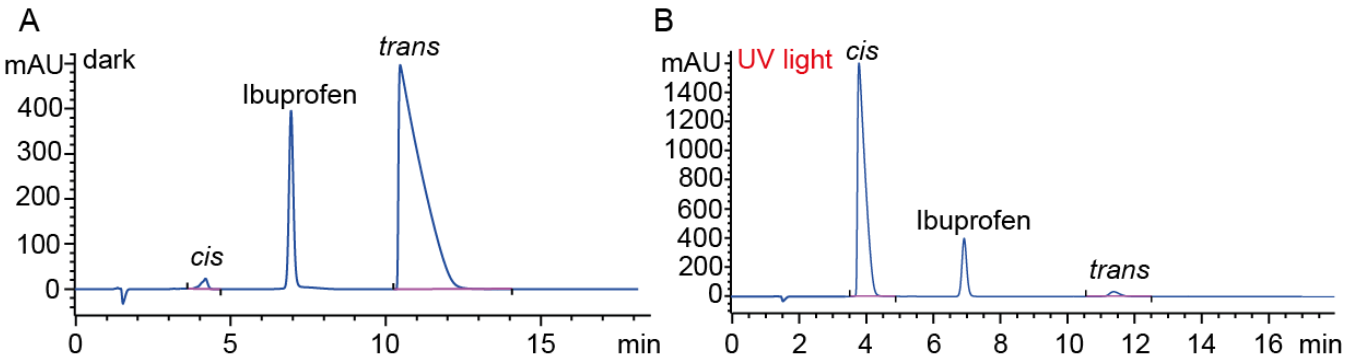

Figure S17. (A) HPLC chromatograms of P^+-Ibuprofen in dark and (B) after UV light irradiation. The area under the peaks was used to calculate the ratio of the *cis* to *trans* form (**Figure S18**).

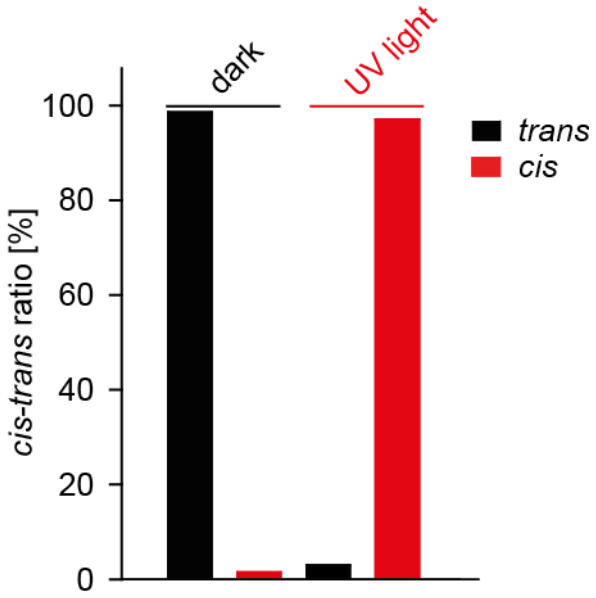

Figure S18. In dark 99% of the molecules were in *trans* state and only 1% in *cis*. After UV light irradiation 3% were in *trans* state and 97% of the molecules were in *cis* state.

Critical micelle concentration (CMC) by isothermal titration calorimetry

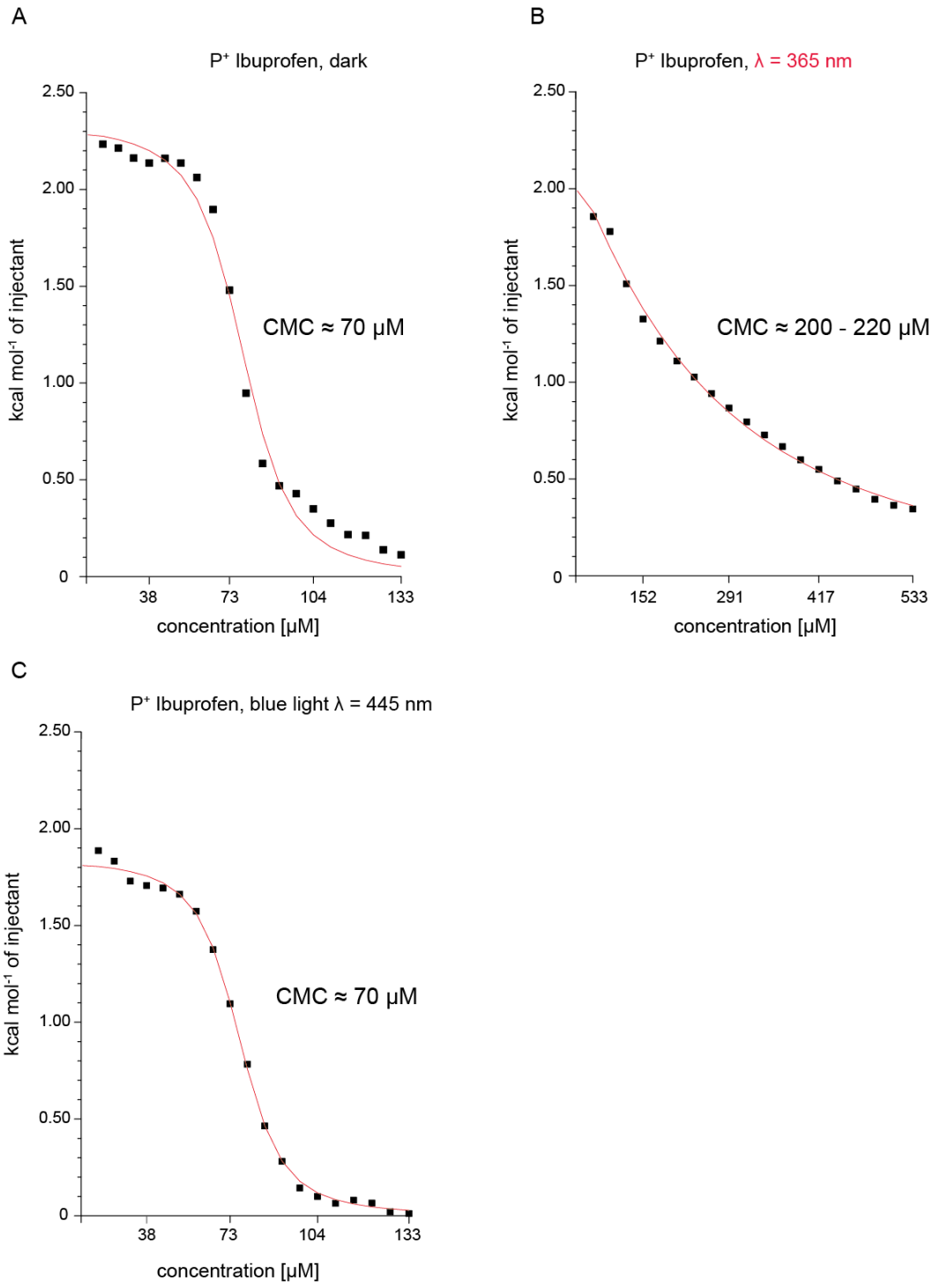

Figure S19. Isothermal titration calorimetry (ITC) data of P+ Ibuprofen in water. The raw data were integrated, the obtained heat changes upon titration were plotted and the data were fitted using a one site model. The ITC raw data were integrated to calculate the heat of each injection of the concentrated stock solutions into pure water. The enthalpy before the critical micelle concentration (CMC) consisted of dilution and de-micellization of the supramolecular species and dilution of the monomers, therefore a higher amount of heat absorption was observed. At CMC the heat per injection dropped limited to the heat of dilution with monomers and micelles in equilibrium. The process was endothermic at 25 °C. The CMC was dependent of the *cis*- to-*trans* ratio of the counterion. After UV light irradiation (97% *cis*) the CMC was increased to about 200 µM compared to 70 µM for the dark state (99% *trans*) and after blue light irradiation (about 80% *trans*).

Concentration dependent UV-VIS spectroscopy

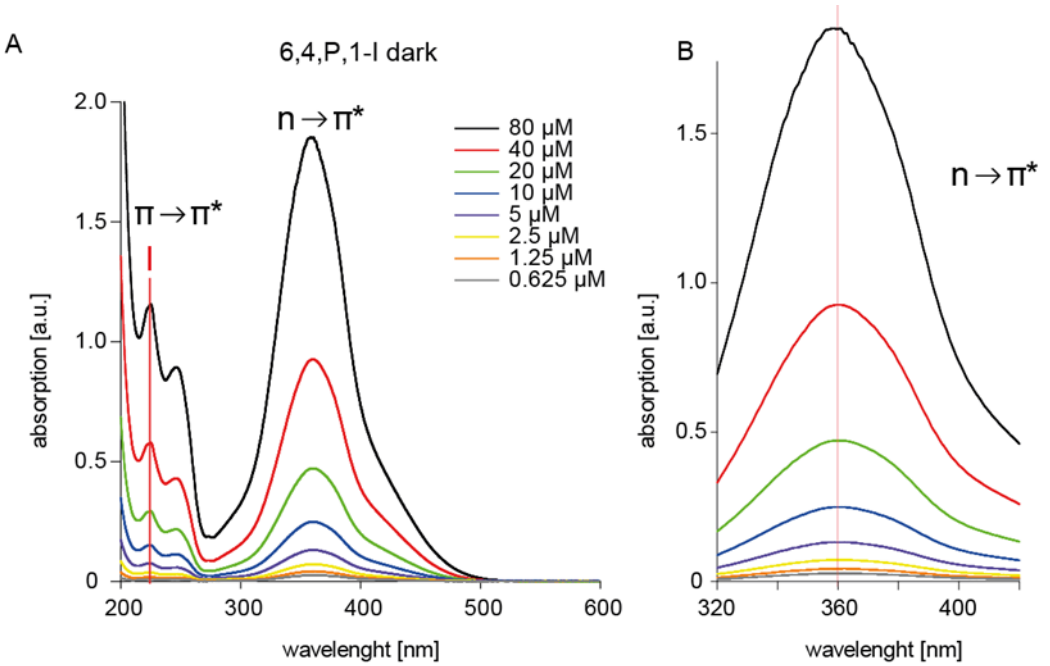

Figure S20. Concentration dependent UV-VIS spectra of P^+-Ibuprofen (dark) in water. After exceeding the CMC of 70 µM the n->π* band shifted hypsochromic as observed during the formation of H-aggregates.

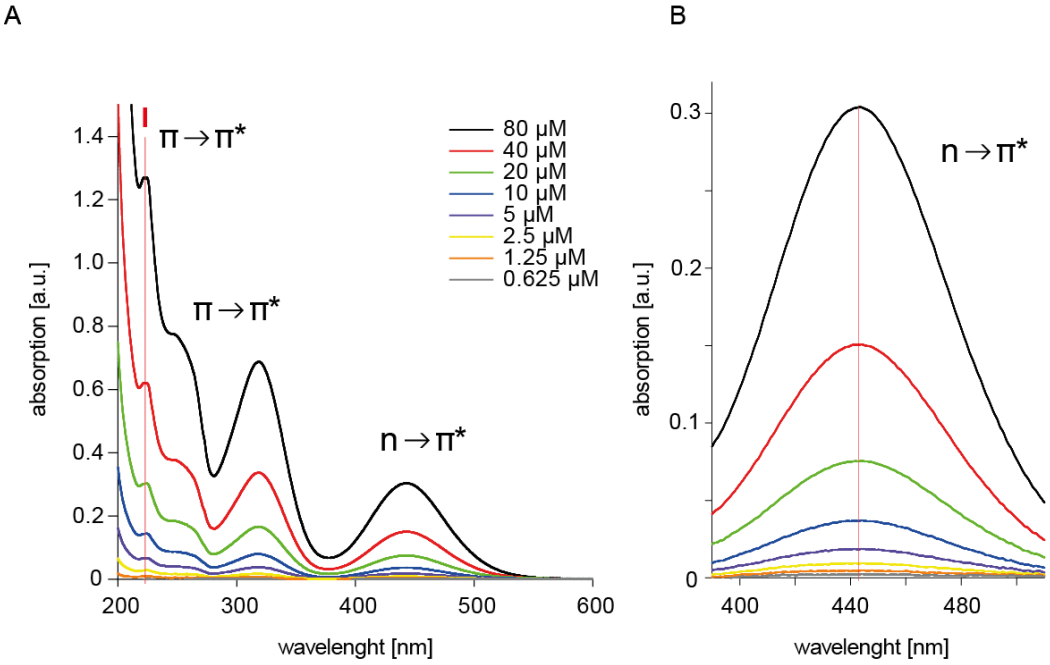

Figure S21. Concentration dependent UV-VIS spectra of P^+-Ibuprofen after 15 min UV light irradiation in water. No shift of the n->π* band was observed, because the CMC of the *cis*-isomer (200 µM) was not exceeded.

Kinetic of the *cis*-to-*trans* isomerization at room temperature in dark

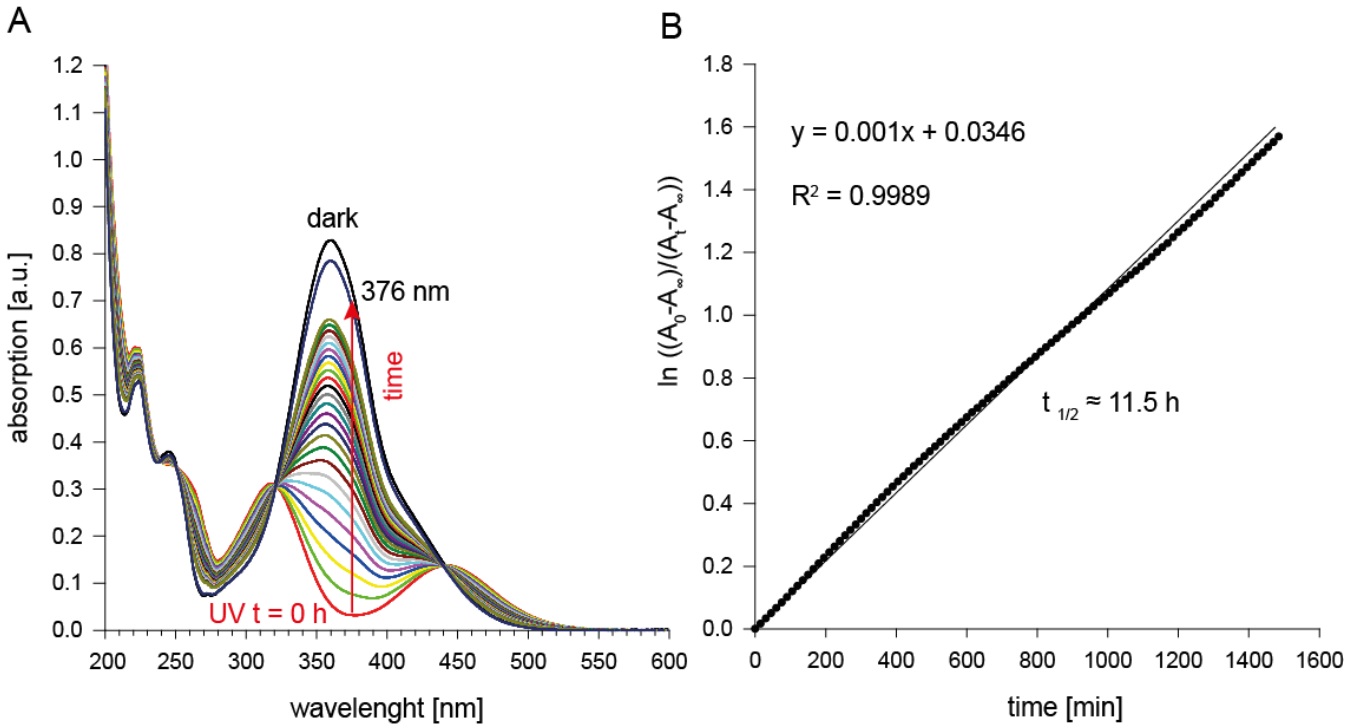

Figure S22. (A) UV-VIS spectra of 40 µM P^+-Ibuprofen in water in dark and immediately after UV light exposure (t = 0 h) overlaid with annually recorded spectra every hour within 24 h and after 48 h stored in the dark at room temperature (20 °C). (B) The absorption A_t at the wavelength of 376 nm was used to calculate the halftime of the *cis* isomer. The *cis*-to-*trans* isomerization followed a first-order kinetic plotting ln ((A0-A∞)/(At-A∞)) against the time [min]. The half time was about 693 min (~ 11.5 h) using the equation ln 2/k and k = 0.001.

Dynamic light scattering (DLS)

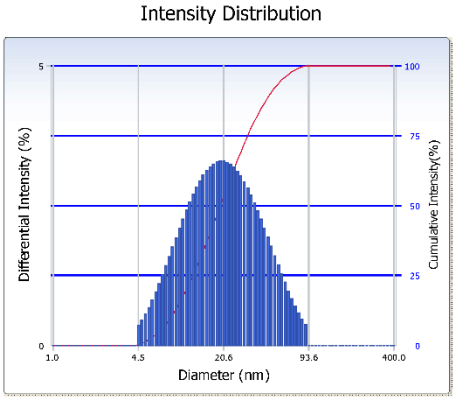

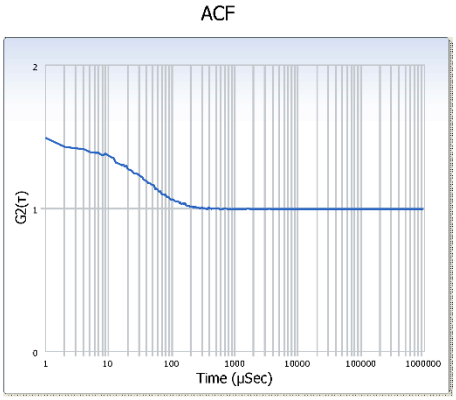

Distribution Results (Contin)

Peak	Diameter (nm)	Std. Dev.
1	24.8	16.6
2	0.0	0.0
3	0.0	0.0
4	0.0	0.0
5	0.0	0.0
Average	24.8	16.6

Residual : 5.907e-003 (O.K)

Cumulants Results

Diameter	(d)	: 16.7	(nm)
Polydispersity Index	(P.I.)	: 0.287	
Diffusion Const.	(D)	: 1.795e-007	(cm²/sec)

Measurement Condition

Temperature	: 25.0	(°C)
Diluent Name	: WATER	
Refractive Index	: 1.3333	
Viscosity	: 1.4600	(cP)
Scattering Intensity	: 9851	(cps)

Figure S23. Dynamic light scattering analysis of a 8 mM P⁺-Ibuprofen solution in water not irradiated (dark).

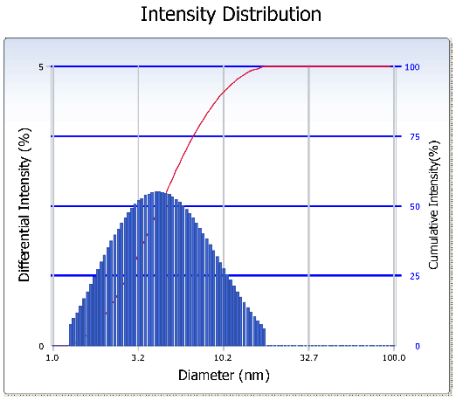

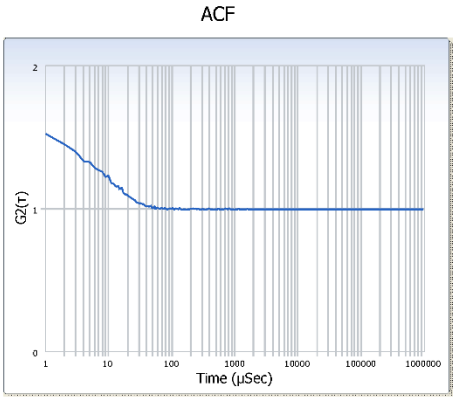

Distribution Results (Contin)

Peak	Diameter (nm)	Std. Dev.
1	5.3	3.3
2	0.0	0.0
3	0.0	0.0
4	0.0	0.0
5	0.0	0.0
Average	5.3	3.3

Residual : 9.136e-003 (O.K)

Cumulants Results

Diameter	(d)	: 4.5	(nm)
Polydispersity Index	(P.I.)	: 0.024	
Diffusion Const.	(D)	: 6.586e-007	(cm²/sec)

Measurement Condition

Temperature	: 25.0	(°C)
Diluent Name	: WATER	
Refractive Index	: 1.3333	
Viscosity	: 1.4600	(cP)
Scattering Intensity	: 9247	(cps)

Figure S24. Dynamic light scattering analysis of a 8 mM P⁺-Ibuprofen solution in water after UV light irradiation.

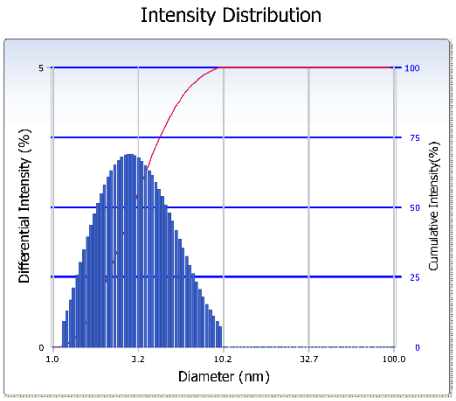

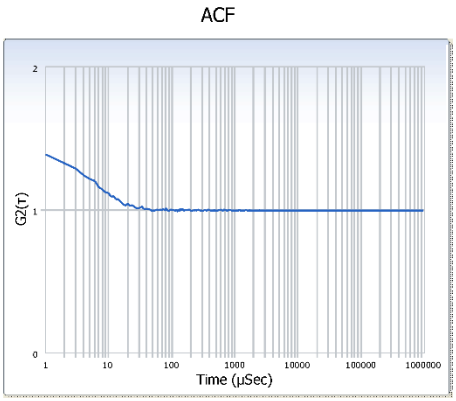

Distribution Results (Contin)

Peak	Diameter (nm)	Std. Dev.
1	3.5	1.8
2	0.0	0.0
3	0.0	0.0
4	0.0	0.0
5	0.0	0.0
Average	3.5	1.8

Residual : 6.433e-003 (O.K)

Cumulants Results

Diameter	(d)	: 3.2	(nm)
Polydispersity Index	(P.I.)	: 0.013	
Diffusion Const.	(D)	: 9.315e-007	(cm^2/sec)

Measurement Condition

Temperature	: 25.0	(°C)
Diluent Name	: WATER	
Refractive Index	: 1.3333	
Viscosity	: 1.4600	(cP)
Scattering Intensity	: 9855	(cps)

Figure S25. Dynamic light scattering analysis of a 8 mM P^+-Ibuprofen solution in water 6 h after UV light irradiation and storage in the dark.

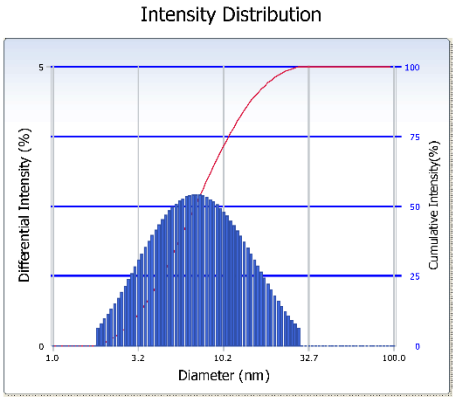

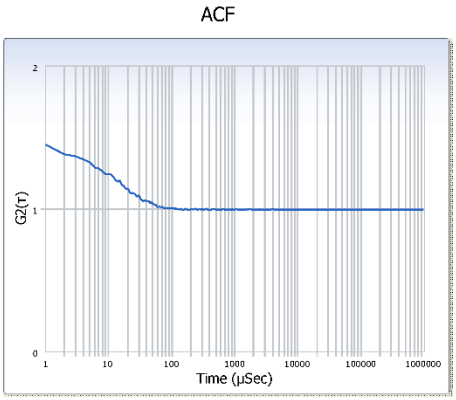

Distribution Results (Contin)

Peak	Diameter (nm)	Std. Dev.
1	8.6	5.4
2	0.0	0.0
3	0.0	0.0
4	0.0	0.0
5	0.0	0.0
Average	8.6	5.4

Residual : 6.743e-003 (O.K)

Cumulants Results

Diameter	(d)	: 7.2	(nm)
Polydispersity Index	(P.I.)	: 0.074	
Diffusion Const.	(D)	: 4.180e-007	(cm^2/sec)

Measurement Condition

Temperature	: 25.0	(°C)
Diluent Name	: WATER	
Refractive Index	: 1.3333	
Viscosity	: 1.4600	(cP)
Scattering Intensity	: 9725	(cps)

Figure S26. Dynamic light scattering analysis of a 8 mM P^+-Ibuprofen solution in water 24 h after UV light irradiation and storage in the dark.

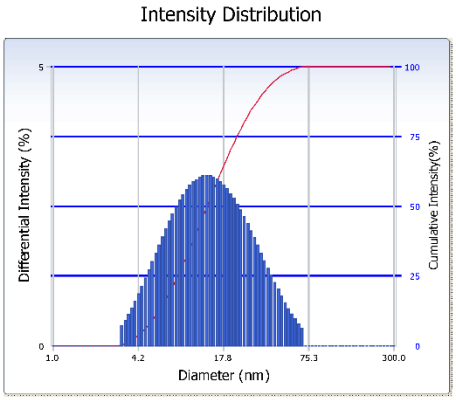

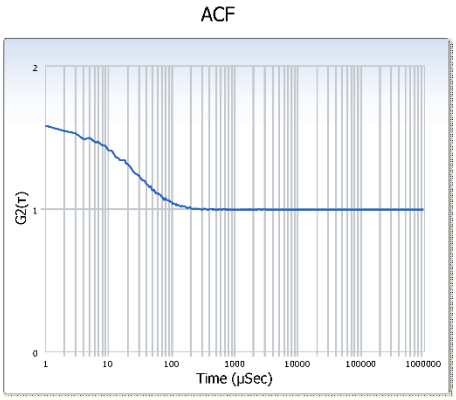

Distribution Results (Contin)

Peak	Diameter (nm)	Std. Dev.
1	17.6	12.4
2	0.0	0.0
3	0.0	0.0
4	0.0	0.0
5	0.0	0.0
Average	17.6	12.4

Residual : 6.521e-003 (O.K)

Cumulants Results

Diameter	(d)	: 11.1	(nm)
Polydispersity Index	(P.I.)	: 0.331	
Diffusion Const.	(D)	: 2.683e-007	(cm^2/sec)

Measurement Condition

Temperature	: 25.0	(°C)
Diluent Name	: WATER	
Refractive Index	: 1.3333	
Viscosity	: 1.4600	(cP)
Scattering Intensity	: 10101	(cps)

Figure S27. Dynamic light scattering analysis of a 8 mM P^+-Ibuprofen solution in water 48 h after UV light irradiation and storage in the dark.

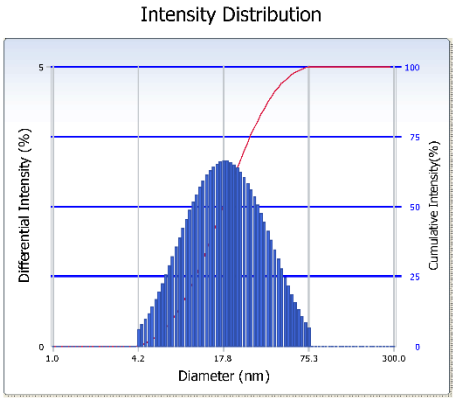

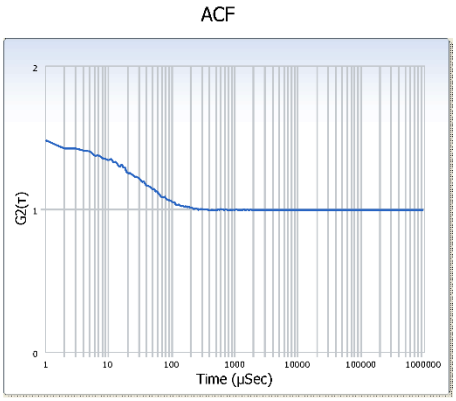

Distribution Results (Contin)

Peak	Diameter (nm)	Std. Dev.
1	22.0	14.0
2	0.0	0.0
3	0.0	0.0
4	0.0	0.0
5	0.0	0.0
Average	22.0	14.0

Residual : 5.942e-003 (O.K)

Cumulants Results

Diameter	(d)	: 13.7	(nm)
Polydispersity Index	(P.I.)	: 0.368	
Diffusion Const.	(D)	: 2.185e-007	(cm^2/sec)

Measurement Condition

Temperature	: 25.0	(°C)
Diluent Name	: WATER	
Refractive Index	: 1.3333	
Viscosity	: 1.4600	(cP)
Scattering Intensity	: 10336	(cps)

Figure S28. Dynamic light scattering analysis of a 8 mM P^+-Ibuprofen solution in water 72 h after UV light irradiation and storage in the dark.

Cryo-transmission electron microscopy

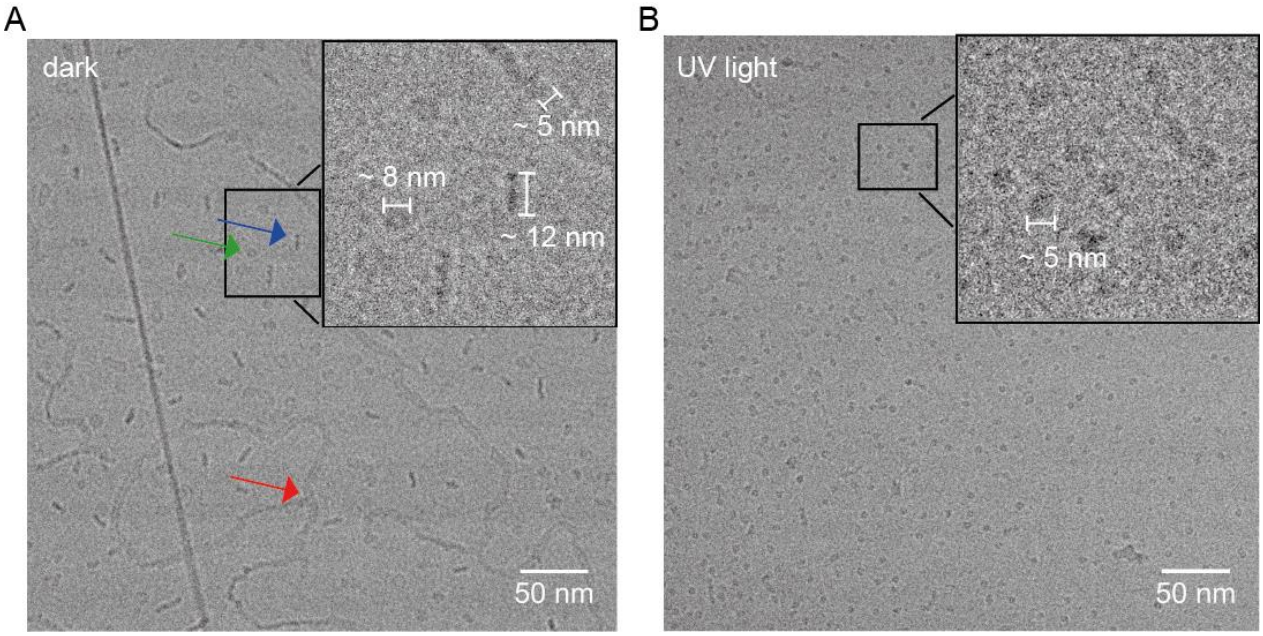

Figure S29. (A) Cryo-transmission electron microscopy images of a 8 mM aqueous solution of P^+-Ibuprofen in dark. Disklike (green arrow), rodlike (blue arrow) and entangled wormlike (red arrow) supramolecular species were visible. (B) After UV light irradiation only small globular mixed micelles were visible.

^{1}H NMR spectra in water of *trans* form

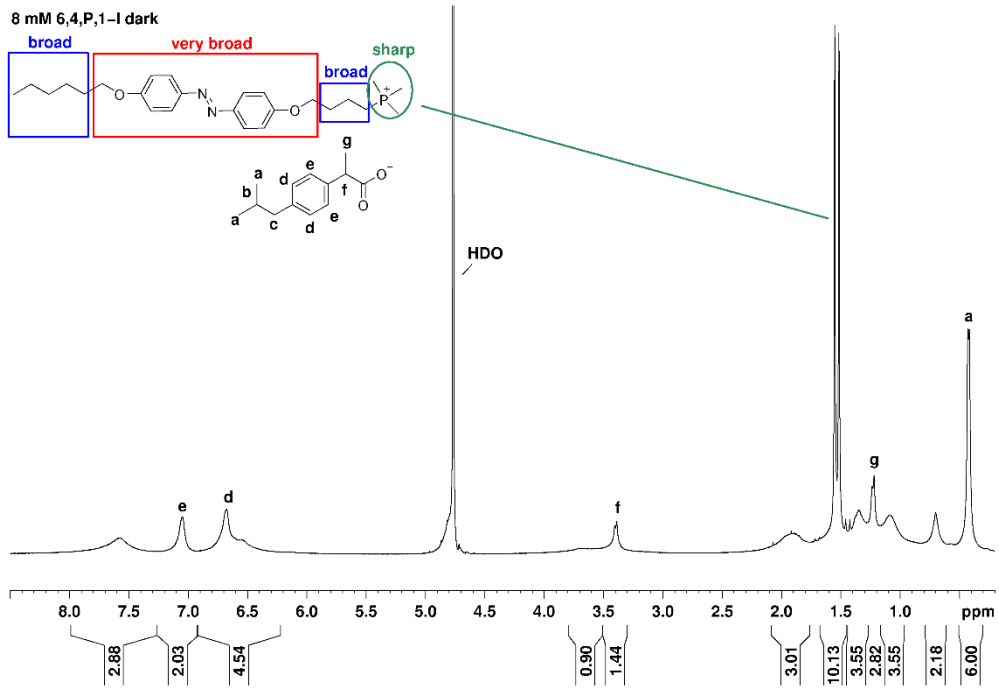

Figure S30. ^{1}H NMR spectrum of 8 mM P$^+$-Ibuprofen dark in deuterated water. The shape of the methyl groups at the polar head of the photoswitchable counterion were sharp (green circle), whereas the shape of the protons of the lipophilic tail (blue box) and especially of the aromatic core (red box) were broad and very broad, respectively. The amphiphilic structure of the counterion resulted in the formation of wormlike supramolecular species, in which the polar phosphonium head showed to the aqueous phase. Due the *π*-*π*-stacking of the aromatic functions of the azobenzene core unit the tumbling rate of the molecules within the micellar structure was strongly reduced explaining the very broad ^{1}H signals. The proton resonances of Ibuprofen were also broaden indicating the arrangement within the micelles.

$^{1}H,^{1}H$-NOESY NMR spectra of *trans* form

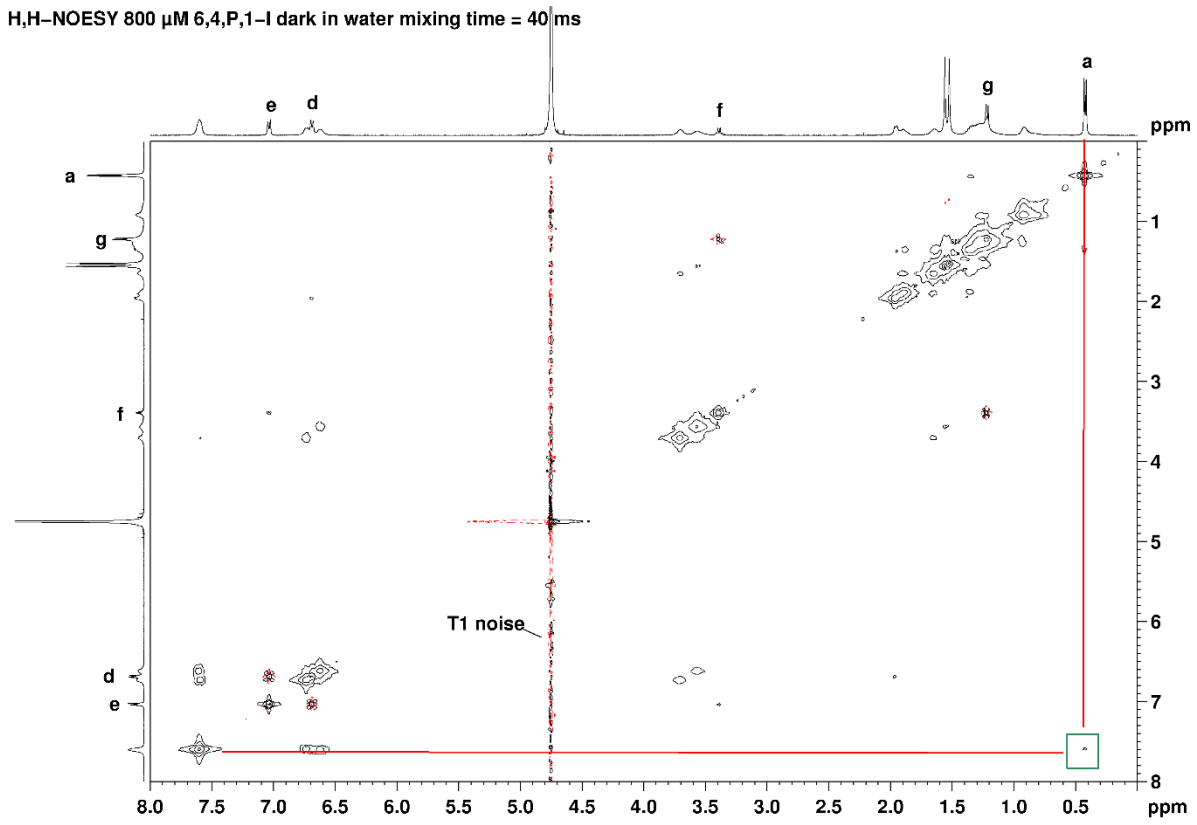

Figure S31. ^{1}H-^{1}H-NOESY of 800 µM P^{+}-Ibuprofen dark dissolved in D_2O. A cross peak (green box) between the isobutyl group of Ibuprofen (a) and the aromatic function of the counterion was detected indicating a close spatial arrangement and penetrating property of the Ibuprofen molecules within the supramolecular species in water.

Molecular modeling of aggregates of *trans* form

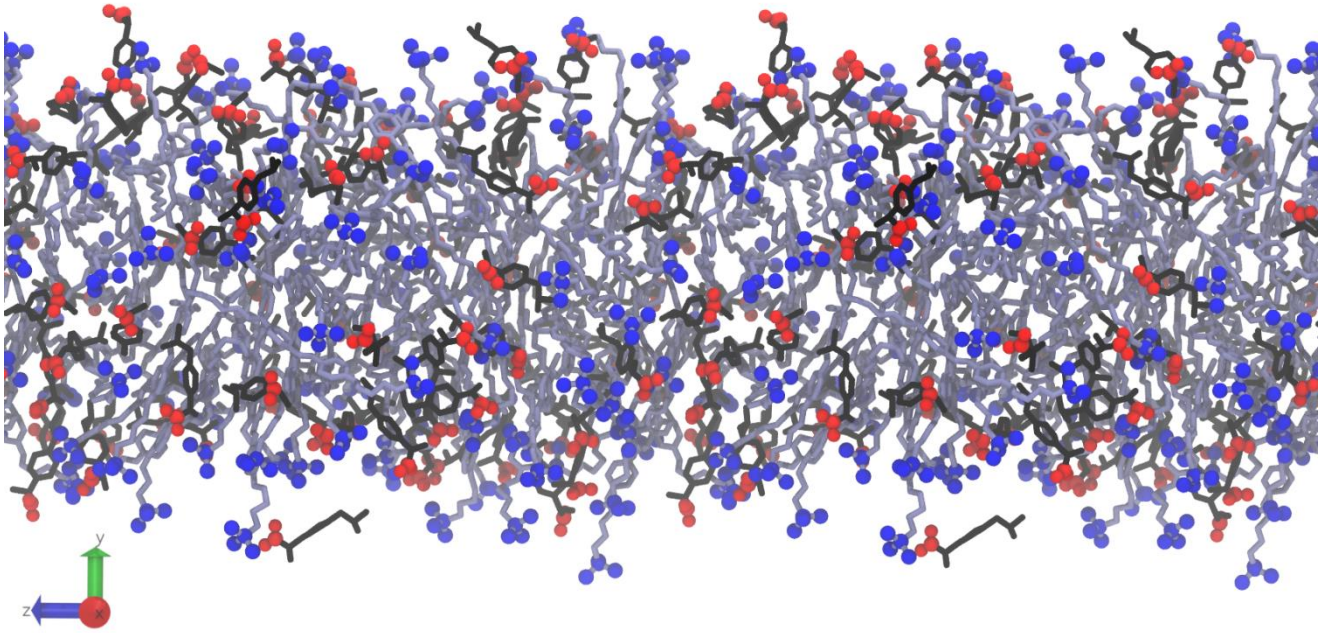

Figure S32. Structure snapshot obtained from MD simulation of a *trans* P^+-azobenzene micelle in the presence of Ibuprofen molecules in aqueous solution. Lipophilic tails of *trans* P^+-azobenzene are shown in ice blue, Ibuprofen is shown in black. Polar head groups of Ibuprofen and P^+-azobenzene are shown as red or blue spheres, respectively. One periodic image and half of each of the neighbouring boxes along the z-axis are shown. For clarity, hydrogen atoms and water molecules, as well as all Ibuprofen molecules in the solvent were hidden.

Upon simulation of the cylindrical *trans* P^+-azobenzene micelle surrounded by an aqueous solution of Ibuprofen, the Ibuprofen molecules quickly entered the micelle, as seen in the illustrated snapshot. Only a few remained in the solvent, and steady exchange between the two phases was observed over time. A continuous worm-like aggregate was maintained during the simulation. A very stable minimum distance of about 0.4 nm between the outer aromatic ring of *trans* P^+-azobenzene and the isobutyl chain of Ibuprofen agrees with observations from the ^{1}H-^{1}H NOESY NMR spectrum (**Figure S31**). In general, direct interactions between the polar head groups, as well as c*ation–π interactions* between the phosphonium group and the aromatic ring of Ibuprofen can be observed during the simulations (**Figure S33**).

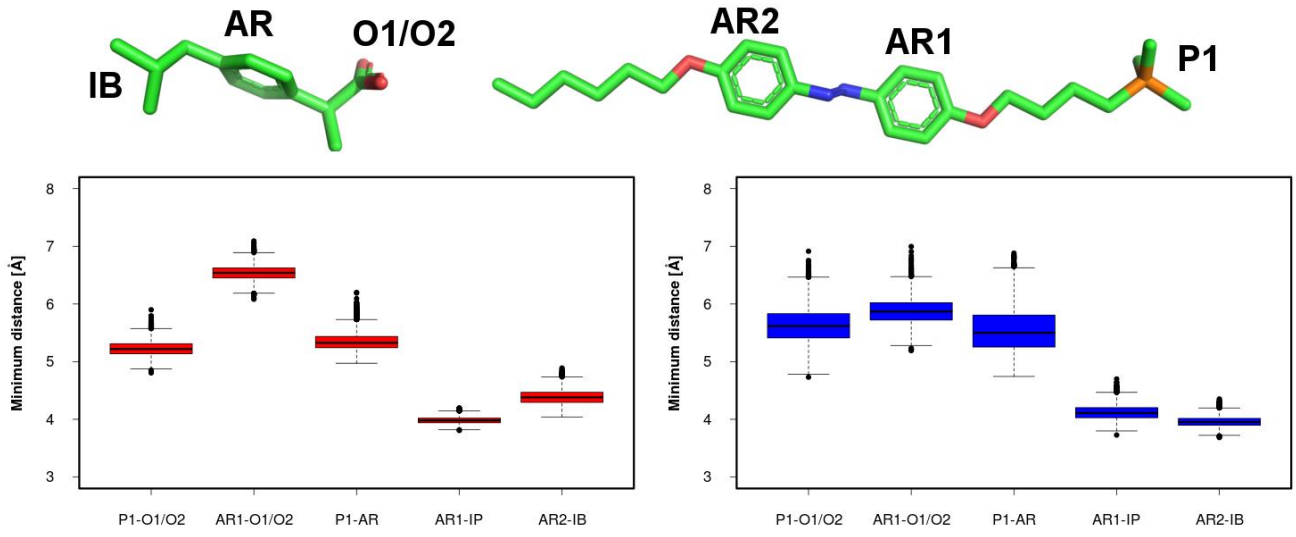

Figure S33. Boxplots for average minimum distances between selected atoms of both simulations (last 5 ns of simulation; AR: benzene rings; O1/O2: Ibuprofen oxygens; IB: isobutyl group of Ibuprofen). Left: wormlike micelle with the *trans* form and Ibuprofen. Right: Globular, small micelle with the *cis* form.

Packing parameter

Table S2: Calculated properties for the packing parameter. Values are given in $nm^1/nm^2/nm^3$. A0: surface area of head group. LH: maximum length of hydrophobic part. V: volume of hydrophobic part. Structures are given for clarification.

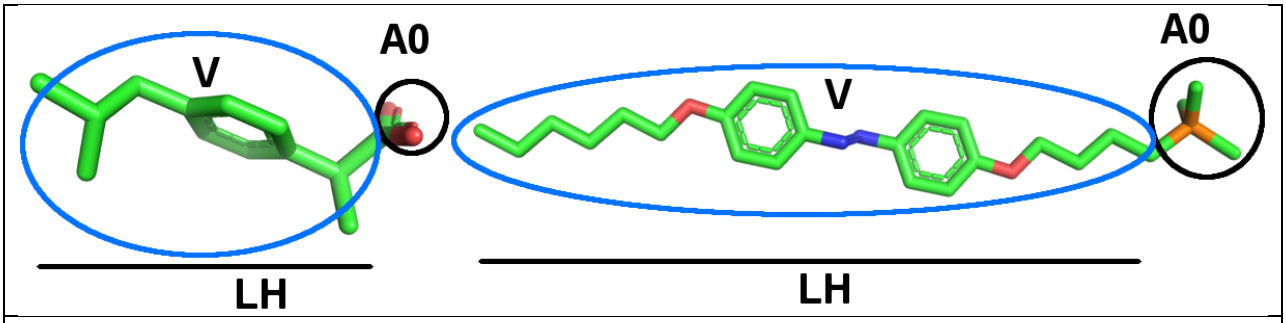

P^+-azobenzene (*trans*)			
measurement	**mean**	**median**	**standard deviation**
A0	0.987	0.974	0.062
LH	2.322	2.329	0.008
V	0.393	0.389	0.011
Ibuprofen			
A0	0.366	0.363	0.024
LH	1.043	1.044	0.002
V	0.202	0.200	0.007

$$packing\ parameter\ P\ for\ trans\ (mean) = \frac{V}{A0 * LH} = \frac{0.393}{0.987 * 2.322} = 0.171$$

$$packing\ parameter\ P\ for\ trans\ (median) = \frac{V}{A0 * LH} = \frac{0.389}{0.974 * 2.329} = 0.171$$

Data for packing parameter calculations given in **Table S2** were calculated from the last 5 ns of the simulation to obtain values for equilibrium conditions. A packing parameter of 0.171 suggests that the system is forming a spherical supramolecular species (P < 0.33). However, in this calculation the counterion effect due to the hydrophobic Ibuprofen molecules is not considered. The repulsive interaction of the positively charged phosphonium groups of the P^+-azobenzene is decreased by intercalation of the Ibuprofen molecules between the P^+-azobenzene molecules, shown by NMR spectroscopy and the simulations. The transition of spherical to rodlike aggregates was described for cetyltrimethylammonium using p-ethyl-benzenesulfonate instead of bromide counterions.[14]

^{1}H NMR spectra in water of *cis* form

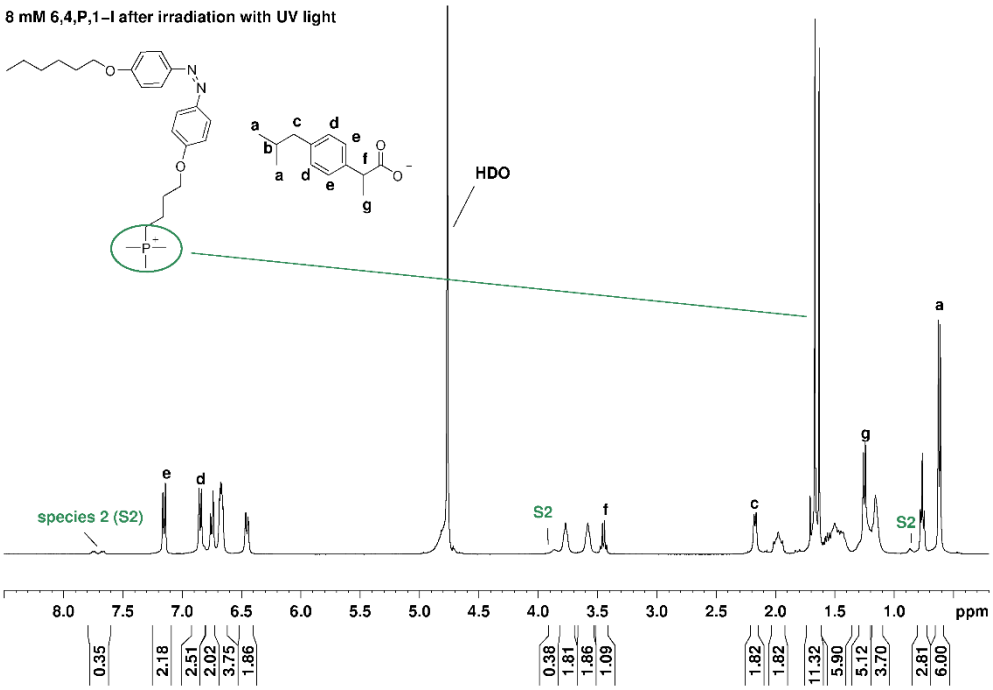

Figure S34. ^{1}H NMR spectrum of 8 mM P^{+}-Ibuprofen after UV light irradiation in deuterated water. The shape of the proton resonances got sharper and a second set of supramolecular species (S2) was detected.

^{1}H,^{1}H-NOESY NMR spectra of *cis* form

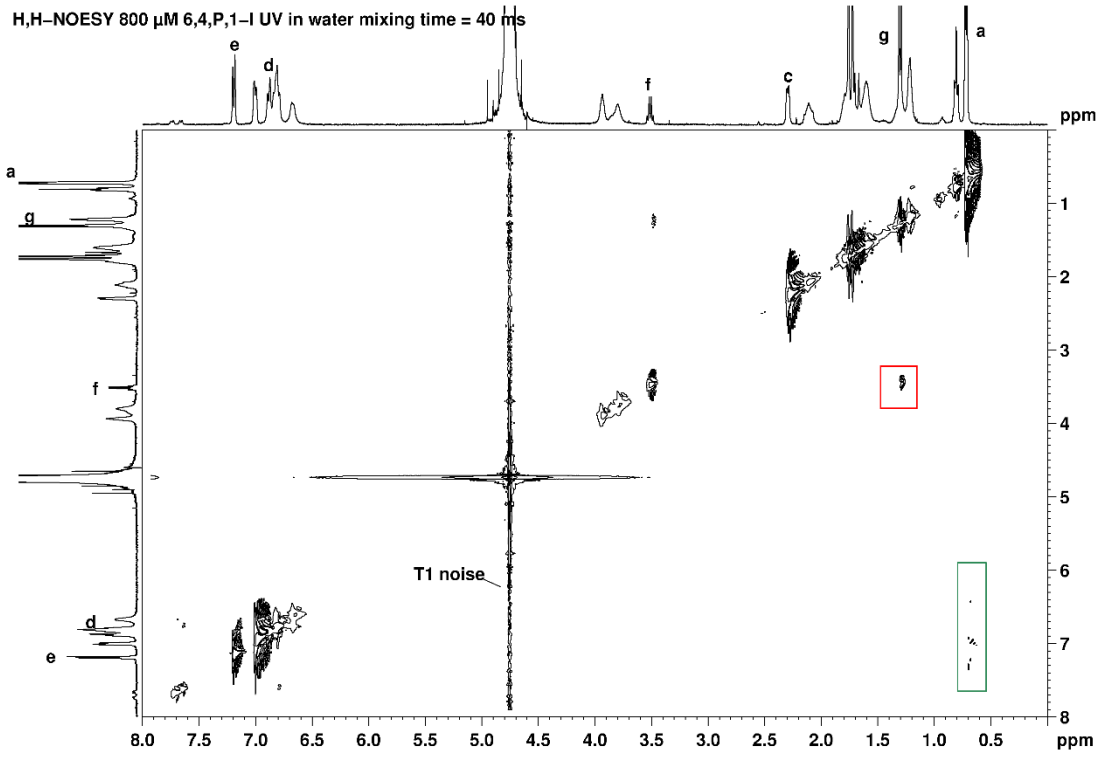

Figure S35. ^{1}H-^{1}H-NOESY of 800 µM P^{+}-Ibuprofen dissolved in D_2O and after UV light irradiation. Due the thermally induced switch back from *cis*-to-*trans* the recording of the NOESY spectra were under dynamic conditions as the ^{1}H signals shifted during the experiment resulting in a distorted spectrum. The cross peaks (green box) of the isobutyl function of Ibuprofen and the aromatic functions of the counterion could indicate an spatial arrangement within the globular, mixed micelles, but the *cis*-to-*trans* isomerization followed by reformation of other supramolecular species aggravated the evaluation of the initial molecular arrangement of the small, globular micelles by NOESY experiments.

Molecular modelling of aggregates of *cis* form

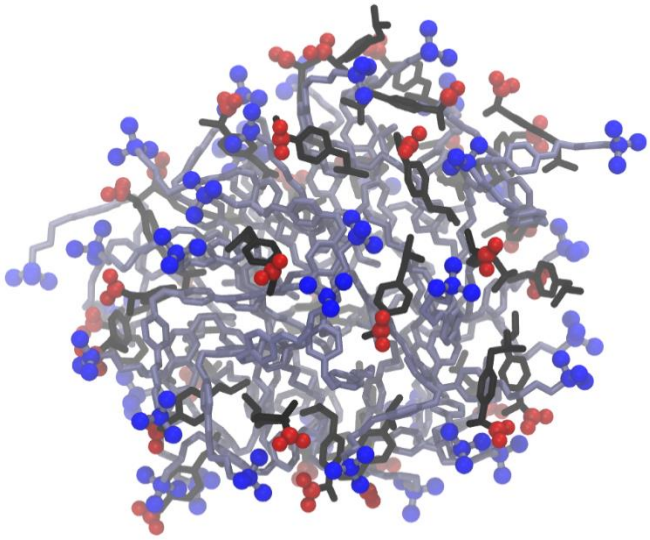

Figure S36. Structure snapshot obtained from MD simulation of a small spherical micelle of *cis* P^+-azobenzene in the presence of Ibuprofen. Lipophilic tails of P^+-azobenzene are shown in ice blue, Ibuprofen is shown in black. Polar head groups of Ibuprofen and P^+-azobenzene are shown as red or blue spheres, respectively. For clarity, hydrogens and water molecules are hidden.

For the spherical micelle of *cis* P^+-azobenzene a very compact globular form without any diffusion of Ibuprofen molecules is maintained throughout the simulation, indicating a very stable formation (**Figure S38**). The maximum radius of gyration for the last 5 ns with respect to the phosphorus atoms of *cis* P^+-azobenzene was calculated: The resulting value of 2.646 ± 0.875 nm is close to the radius of about 2.5 nm from cryo-TEM observations. However, since only a single spherical micelle of *cis* P^+-azobenzene was built, with an arbitrarily chosen amount of 72 molecules, the simulation result should be treated with caution. Minimum distances show a slightly broader distribution than in the *trans* P^+-azobenzene micelle (**Figure S33**). The isobutyl group is shifted more towards the inner aromatic ring of *cis* P^+-azobenzene, and the distance of the carboxylate to the outer ring is shortened, as Ibuprofen is able to occupy the space between the aromatic moieties of *cis* P^+-azobenzene.

Scanning laser transformation

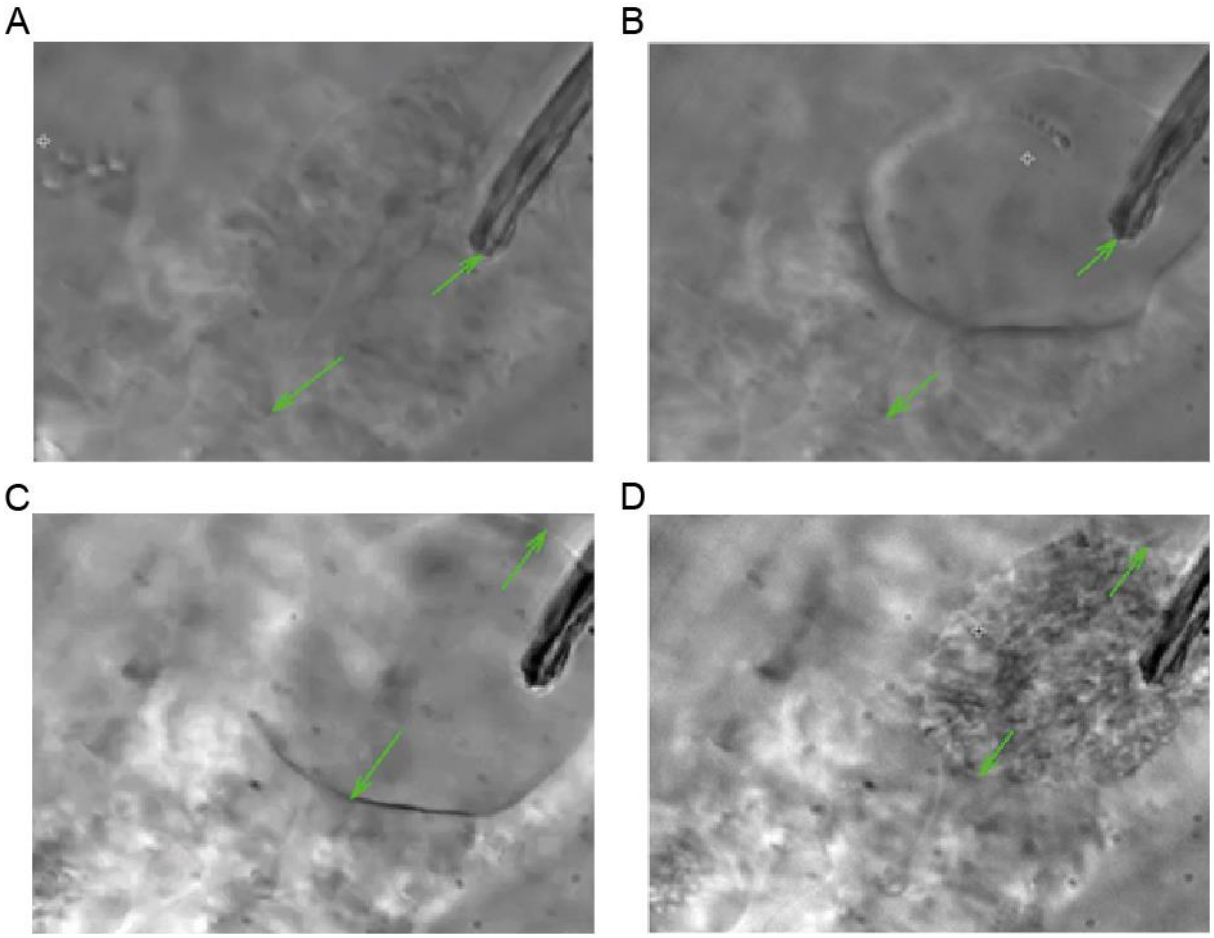

Figure S37. Effects of focused laser light on photoswitchable hydrogel of P^+-Ibuprofen. (A) Gel before irradiation with scanned 730 nm 80 mW femtosecond laser for two-photon conversion. The objective lens was 60x 0.65 NA. Green arrows mark fiducial points in gel. (B) Gel after scanning with femtosecond laser. The spacing between fiducial points has increased by a factor of 1.11. (C) Expanded gel before illumination with scanned 5 mW 532 nm continuous wave laser. D) Restoration of structure and shrinkage by factor of 0.9 after scanning illumination. These images are stills from **Video S2**.

***In vitro* cytotoxicity**

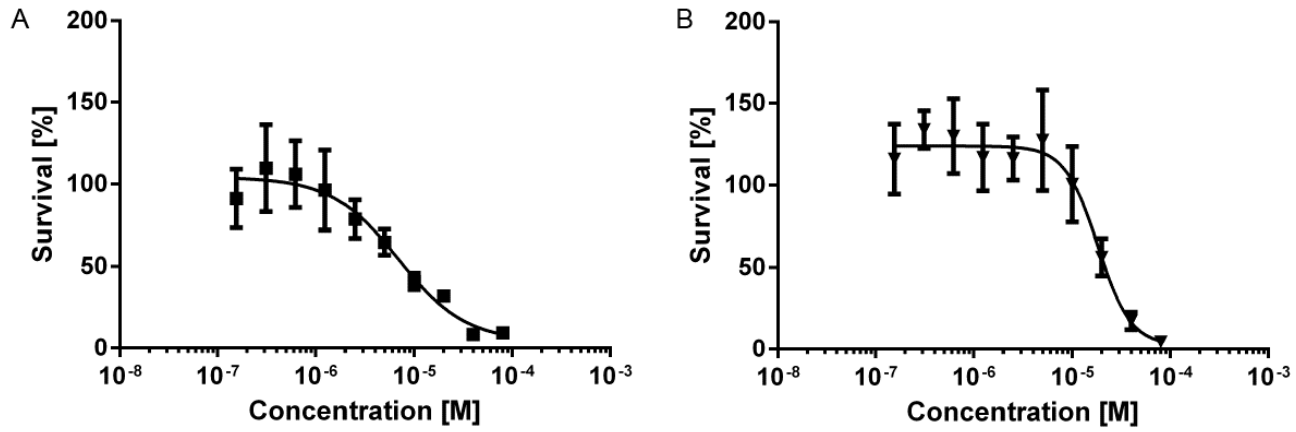

Figure S38. Cytotoxicity WST-1 assay of the photoswitchable counterion as bromide salts shown in **Figure 1A** with (A) being the ammonium azobenzene (IC_{50} = 7 µM) and (B) being the phosphonium azobenzene (IC_{50} = 18 µM) with HaCaT cells p47.

References

1. Wang, Z.; Larson, R. G., Molecular dynamics simulations of threadlike cetyltrimethylammonium chloride micelles: effects of sodium chloride and sodium salicylate salts. *J Phys Chem B* **2009,** *113* (42), 13697-710.
2. Yan, H.; Han, Z.; Li, K.; Li, G.; Wei, X., Molecular Dynamics Simulation of the pH-Induced Structural Transitions in CTAB/NaSal Solution. *Langmuir* **2018,** *34* (1), 351-358.
3. Jorgensen, W. L.; Chandrasekhar, J.; Madura, J. D.; Impey, R. W.; Klein, M. L., Comparison of simple potential functions for simulating liquid water. *J. Chem. Phys.* **1983,** *79*, 926-935.
4. Case, D. A.; Ben-Shalom, I. Y.; Brozell, S. R.; Cerutti, D. S.; Cheatham, T. E., III; Cruzeiro, V. W. D.; Darden, T. A.; Duke, R. E.; Ghoreishi, D.; Gilson, M. K.; Gohlke, H.; Goetz, A. W.; Greene, D.; Harris, R.; Homeyer, N.; Izadi, S.; Kovalenko, A.; Kurtzman, T.; Lee, T. S.; LeGrand, S.; Li, P.; Lin, C.; Liu, J.; Luchko, T.; Luo, R.; Mermelstein, D. J.; Merz, K. M.; Miao, Y.; Monard, G.; Nguyen, C.; Nguyen, H.; Omelyan, I.; Onufriev, A.; Pan, F.; Qi, R.; Roe, D. R.; Roitberg, A.; Sagui, C.; Schott-Verdugo, S.; Shen, J.; Simmerling, C. L.; Smith, J.; Salomon-Ferrer, R.; Swails, J.; Walker, R. C.; Wang, J.; Wei, H.; Wolf, R. M.; Wu, X.; Xiao, L.; York, D. M.; Kollman, P. A. , *AMBER* **2018,** *University of California*, San Francisco.
5. Chemical Computing Group ULC. *Molecular Operating Environment (MOE)* **2018**, Montreal, Quebec.
6. Frisch, M. J.; Trucks, G. W.; Schlegel, H. B.; Scuseria, G. E.; Robb, M. A.; Cheeseman, J. R.; Scalmani, G.; Barone, V.; Petersson, G. A.; Nakatsuji, H.; Li, X.; Caricato, M.; Marenich, A. V.; Bloino, J.; Janesko, B. G.; Gomperts, R.; Mennucci, B.; Hratchian, H. P.; Ortiz, J. V.; Izmaylov, A. F.; Sonnenberg, J. L.; Williams-Young, D.; Ding, F.; Lipparini, F.; Egidi, F.; Goings, J.; Peng, B.; Petrone, A.; Henderson, T.; Ranasinghe, D.; Zakrzewski, V. G.; Gao, J.; Rega, N.; Zheng, G.; Liang, W.; Hada, M.; Ehara, M.; Toyota, K.; Fukuda, R.; Hasegawa, J.; Ishida, M.; Nakajima, T.; Honda, Y.; Kitao, O.; Nakai, H.; Vreven, T.; Throssell, K.; Montgomery, J. A., Jr.; Peralta, J. E.; Ogliaro, F.; Bearpark, M. J.; Heyd, J. J.; Brothers, E. N.; Kudin, K. N.; Staroverov, V. N.; Keith, T. A.; Kobayashi, R.; Normand, J.; Raghavachari, K.; Rendell, A. P.; Burant, J. C.; Iyengar, S. S.; Tomasi, J.; Cossi, M.; Millam, J. M.; Klene, M.; Adamo, C.; Cammi, R.; Ochterski, J. W.; Martin, R. L.; Morokuma, K.; Farkas, O.; Foresman, J. B.; Fox, D. J., *Gaussian 09, Revision C.01* **2016**, Gaussian, Inc., Wallingford CT.
7. Wang, J.; Wolf, R. M.; Caldwell, J. W.; Kollman, P. A.; Case, D. A., Development and testing of a general amber force field. *J Comput Chem* **2004,** *25* (9), 1157-74.
8. Duchstein, P.; Neiss, C.; Gorling, A.; Zahn, D., Molecular mechanics modeling of azobenzene-based photoswitches. *J Mol Model* **2012,** *18* (6), 2479-82.
9. Bockmann, M.; Peter, C.; Site, L. D.; Doltsinis, N. L.; Kremer, K.; Marx, D., Atomistic Force Field for Azobenzene Compounds Adapted for QM/MM Simulations with Applications to Liquids and Liquid Crystals. *J Chem Theory Comput* **2007,** *3* (5), 1789-802.
10. Phillips, J. C.; Braun, R.; Wang, W.; Gumbart, J.; Tajkhorshid, E.; Villa, E.; Chipot, C.; Skeel, R. D.; Kale, L.; Schulten, K., Scalable molecular dynamics with NAMD. *J Comput Chem* **2005,** *26* (16), 1781-802.
11. Darden, T.; York, D.; Pedersen, L., Particle mesh Ewald: An N·log(N) method for Ewald sums in large systems *J. Chem. Phys.* **1993,** *98*, 10089-10092.
12. Israelachvili, J. N.; Mitchell, D. J.; Ninham, B. W., Theory of self-assembly of hydrocarbon amphiphiles into micelles and bilayers. *J. Chem. Soc., Faraday Trans. 2* **1976,** *72*, 1525-1568.
13. Humphrey, W.; Dalke, A.; Schulten, K., VMD: visual molecular dynamics. *J Mol Graph* **1996,** *14* (1), 33-8, 27-8.
14. Gamboa, C.; Rios, H.; Sepulveda, L., Effect of the Nature of Counterions on the Sphere-to-Rod Transition In Cetyltrimethylammonium Micelles. *J. Phys. Chem.* **1989,** *93*, 5540-5543.
15. Scherrer, P., Bestimmung der inneren Struktur und der Größe von Kolloidteilchen mittels Röntgenstrahlen. *Kolloidchemie Ein Lehrbuch* **1912**, 387–409.
16. de Jeu, W., Basic X-Ray Scattering for Soft Matter. *Oxford University Press* **2016**.